PHILOSOPHICAL TRANSACTIONS OF THE ROYAL SOCIETY A MATHEMATICAL, PHYSICAL & ENGINEERING SCIENCES

The Electronic Emission Spectrum of Ionized Nitrous Oxide, N_{2}O$^{+}: \tilde{A}^{2}\Sigma ^{+}-\tilde{X}^{2}\Pi $

J. H. Callomon and F. Creutzberg

Phil. Trans. R. Soc. Lond. A 1974 **277**, 157-189
doi: 10.1098/rsta.1974.0048

THE ELECTRONIC EMISSION SPECTRUM OF IONIZED NITROUS OXIDE, N_2O^+: $\tilde{A}\,^2\Sigma^+$–$\tilde{X}\,^2\Pi$

By J. H. Callomon and F. Creutzberg†
Chemistry Department, University College London, Gower Street, London, WC1H 0AJ

(*Communicated by D. P. Craig, F.R.S. – Received 31 December 1973*)

[Plates 4 and 5]

CONTENTS

	PAGE
1. Introduction	158
2. Experimental	159
(*a*) Materials	159
(*b*) Optical	159
3. Analysis	160
(*a*) Rotational analysis	162
(*b*) Electronic orbital and spin terms	167
(*c*) Vibrational analysis: stretching vibrations ν_1, ν_3	169
(*d*) Bending vibrations and Renner–Teller coupling	172
(*e*) Perturbations	175
4. Molecular structure	177
(*a*) Bond distances	177
(*b*) Force constants	178
(*c*) Dissociation limits, predissociation and products	182
(*d*) Electronic structure	183
References	184
Appendix: Wavelengths and frequencies of band heads in the spectra of $N_2{}^{16}O^+$ and $N_2{}^{18}O^+$	186

The emission spectrum of the transition $\tilde{A}\,^2\Sigma^+$–$\tilde{X}\,^2\Pi$ between the two lowest states of the ion of N_2O have been photographed under high resolution and analysed in both of the two isotopes $N_2{}^{16}O^+$ and $N_2{}^{18}O^+$.

The principal vibrational structure yields the stretching fundamentals in both states (table 11), from which complete sets of quadratic valence stretching force constants are obtained, albeit uncorrected for anharmonicities (table 14). The excited state $\tilde{A}\,^2\Sigma$ is more tightly bound than the neutral N_2O in its ground state.

Sequences in the bending vibration show the effects of moderate Renner–Teller vibronic coupling in the orbitally degenerate $^2\Pi$-state ($\epsilon = -0.19$); and together with a few weaker bands of different polarization involving $\Delta v_2 = \pm 1$ observed presumably through Herzberg–Teller vibronic coupling, these transitions make possible a

† Present address: Astrophysics Branch, National Research Council of Canada, Montreal Road, Ottawa K1A OR8, Ontario.

complete analysis of the Renner coupling in $v_2'' = 1$ (table 10) and hence yield the bending frequencies and force constants. This analysis provides one of the best tests so far of the Renner–Pople–Hougen theory of these couplings.

Rotational analysis gives zero-point moments of inertia I_0 from which r_0-structures are calculated for both states (table 13). Finally, the force constants and bond distances of the ion are compared with those of the neutral molecule, and the states of the ion correlated with those of possible dissociation products (table 16).

1. Introduction

The emission spectrum of N_2O^+ was first observed simultaneously in three different sources: during X-ray irradiation of N_2O (Brocklehurst 1958); during controlled electron bombardment of N_2O (Horani & Leach 1959), and from the negative glow in the hollow cathode of a d.c. discharge through N_2O (Callomon 1959). The spectra in the first two sources are relatively free of those of impurities but weak. Those from the hollow cathode are intense enough to be photographed under high dispersion but under normal conditions are badly overlapped by bands of N_2, N_2^+ and NO. A rotational analysis was therefore initially made only of the zero–zero band.

In the course of measuring the radiative life-time of the spectrum (Dayton, Dalby & Bennett 1960) some greatly improved spectra were obtained. These were analysed vibrationally and in some of the stronger bands rotationally by Abernethy (1964). Besides the perpendicularly polarized bands of the main system he identified also some weak bands of parallel polarization involving changes of single quanta in the bending vibration and thus made the first estimates of some of the vibronic interaction terms associated with the Renner–Teller effect in the degenerate state of the ion.

Table 1. Known states of ionized nitrous oxide

	state	energy/eV		electron configuration	observation†	references‡
N_2O^+	$(\tilde{F})(^2\Pi?)$	~24.3	11.4	$2\pi^2.3\pi^*$	p.e.s.	(*d*)
	$(\tilde{E})(^2\Pi?)$	~22.5	9.6	$2\pi^2.3\pi^*$	p.e.s.	(*d*)
	$\tilde{C}(^2\Sigma)$	20.105	7.212	6σ	4 Rydberg series; p.e.s., p.i.	(*a*) (*b*), (*c*)
	$\tilde{D}(^2\Pi?)$	~19.5	6.6	$2\pi^2.3\pi^*$	p.e.s.	(*d*)
	$\tilde{B}(^2\Pi)$	17.65	4.76	$1\pi^3$	p.e.s.	(*b*)
	$\tilde{A}\,^2\Sigma^+$	16.396	3.503	7σ	2 Rydberg series; $\tilde{A}$–$\tilde{X}$; p.e.s., p.i.	(*a*) (*b*), (*c*), (*f*)
	$\tilde{X}\,^2\Pi_i(a)$	12.893 ≡ 0		$2\pi^3$	2 Rydberg series; p.e.s., p.i., e.s.r.	(*a*) (*b*), (*c*), (*e*)
	...					
N_2O	$\tilde{X}^1\Sigma^+$	0		$KKK4\sigma^25\sigma^26\sigma^21\pi^47\sigma^22\pi^4$		

† p.e.s., photoelectron spectroscopy; p.i., far-u.v. photoionization spectrum; e.s.r., electron spin-resonance in a cold solid.

‡ (*a*) Tanaka, Jursa & LeBlanc (1960); (*b*) Turner & May (1967), Turner *et al.* (1970); (*c*) Dibeler & Walker; (1968); (*d*) Price & Potts, in Lorquet & Cadet (1971); (*e*) Smith & Seddon (1969); (*f*) $\tilde{A}$–$\tilde{X}$, here.

At about the same time much better spectra from the hollow cathode allowed us to extend greatly the range of bands that could be photographed under high resolution and this paper presents the full analysis of the spectra of N_2O^+ and $N_2{}^{18}O^+$ (Creutzberg 1964). Some of the leading constants have been published previously in summary form (in Herzberg 1966, p. 593; Callomon & Creutzberg 1968).

Subsequently, the spectrum has been observed in yet other sources: during collisions between

N_2O and H_2 (Poulizac & Druetta 1969) or Ar^+ (Haugh & Bayes 1970) with high kinetic energies; or as fluorescence from N_2O excited directly into the photoionization continuum with helium resonance-radiation $\lambda = 584$ Å (Monahan & Wauchop 1972). The presence and properties of individual states of the ion of N_2O have also been observed by a variety of methods, and for convenience those data which could not be included in Herzberg's book (1966) will be added to the tables in this paper whenever possible.

Four states of N_2O^+ are now definitely known, with some evidence for three more. Their positions and methods of observation are shown in table 1.

2. Experimental

(*a*) *Materials*

Commercial nitrous oxide of medical quality was used without further purifications to obtain the spectra of $N_2{}^{16}O^+$.

$N_2{}^{18}O$ was prepared by direct oxidation of ammonia with gaseous oxygen on a platinum catalyst. The starting material was 1 g $H_2{}^{18}O$ (Yeda, Rehovoth), and this route was chosen as it involves only two stages: electrolysis of the water, and the oxidation. The water was electrolysed in a microelectrolytic cell which consists essentially of a capillary U-tube with platinum electrodes and pressure equalizing bulbs which also collect the evolved gases. The electrolyte was 0.1 M $Na^{18}OH$ prepared by adding 20 mg of fresh sodium to the water. This was done by distilling the water *in vacuo* into the calculated length of glass capillary of known diameter into which molten sodium had been drawn, broken into small pieces. A current of 60 mA over a day electrolysed about half a gram of water.

Zawadski (1950) has described conditions under which ammonia can be oxidized catalytically to give high yields of N_2O and these were modified for best yields as follows. Platinized asbestos was used instead of palladized asbestos which was wholly unsatisfactory; and the length of the bed of catalyst in a Pyrex tube as reaction chamber was 3 cm. Above 10 cm the yield of oxides of nitrogen falls rapidly. The best yield of N_2O was obtained with a mixture $NH_3:O_2$ of 1:1, but was not sensitive to small deviations from this ratio and unaffected by added nitrogen. The total pressure in the reaction vessel was about 65 Pa. Yields below 280 °C were negligible. That of N_2O rose to a maximum at 360 °C, staying constant up to about 400 °C with progressively higher yields of NO_2 as side-product. The yield at 360 °C of N_2O per cycle was about 56 % of the stoichiometric theoretical, with 5 % of NO_2 and traces of NO. After removing and fractionating the condensible products, NO and unchanged O_2 were fixed on heated copper so that almost all the ^{18}O not converted to N_2O could be recovered as $H_2{}^{18}O$. About 0.1 l atm/h of $N_2{}^{18}O$ was thus prepared with an overall ^{18}O yield of 80 %. Purity was checked spectroscopically and no measurable isotopic degradation had occurred.

(*b*) *Optical*

The hollow cathode source consisted essentially of a water cooled slot 3 mm × 1½ mm × 50 mm in copper (cf. Callomon 1958) and with high flow rates (*ca.* 1 l atm/h) of pure N_2O at minimum currents of *ca.* 7 mA d.c. rectified and unsmoothed from a transformer, spectra of N_2O^+ almost free from impurities were obtained. The flickering discharge could be stabilized by winding a loose coil round the glass limb carrying the positive column and coupling it to a small induction coil. Spectra of $N_2{}^{18}O^+$ were obtained under similar conditions, but to conserve material,

the parent gas was diluted about 1000-fold with helium. The spectra of impurities were then rather more prominent, but not troublesome in the selected regions photographed under high resolution.

Survey spectra for measurements of band heads were photographed in the first and second orders of a Bausch and Lomb $1\frac{1}{2}$ m Eagle spectrograph. Selected strong bands were photographed in the second order of a 6 m Ebert spectrograph with a resolving power of 300000 ($\Delta\bar{\nu} = 0.10$ cm^{-1} at 3500 Å) and with exposures on Kodak Oa-0 plates of between 10 min and 3 h. Spectra were calibrated by fitting wavelengths of lines from an iron arc to a dispersion curve whose nonlinear terms had been calculated with the help of the optical constants of grating and spectrograph, and using line positions measured with an Abbe comparator (Zeiss, Jena). The question of calibration was gone into with some care, for the constants obtained in the present analysis differ by small but significant amounts from those reported previously. We attribute the differences to an effectively progressive screw error in the measuring microscope used earlier, of a kind that cannot occur in the engraved scale of the comparator. The crucial quantity is the difference between the principal rotational constants B_0 of the two isotopic species studied, and care was therefore taken to see that the two (0, 0) bands to be compared were photographed and processed under as closely similar conditions as possible. Independent measurements of different plates of the same bands showed that relative line frequencies were exactly reproducible, and in well resolved branches the scatter of measured frequencies about the values calculated from the constants obtained was 0.004 cm^{-1}.

Note on vibrational numbering. We retain the old-established convention of labelling the lower and higher stretching frequencies ν_1 and ν_3 respectively, by analogy with iso-electronic and centrosymmetric molecules like CO_2. This is the converse of Herzberg's notation (1966). No confusion is likely to arise.

3. Analysis

Two densitometric traces of the spectrum photographed under low resolution on a prism instrument are shown in figure 1. There is a single short but prominent progression in a lower-state frequency of 1126 cm^{-1}, identified as ν_1, with a corresponding upper-state interval of 1345 cm^{-1} of which only the first member is observed. Grouped around the strong bands of these progressions are numerous weaker ones involving the other vibrational modes in sequences and short progressions. Most bands occur in pairs of sub-bands of almost equal intensities, separated by the characteristic spin-orbit splitting of the lower $^2\Pi$ state of 133 cm^{-1}; and each sub-band is double headed, degraded to shorter wavelenths. These bands arise therefore from transitions that are perpendicularly polarized, of type $^2\Sigma$–$^2\Pi(a)$. There are, in addition, a few weaker bands of $^2\Sigma$–$^2\Sigma$ or $^2\Pi$–$^2\Pi$ structure and hence parallel polarization involving $\Delta v_2 = \pm 1$ in the bending vibration.

The (0, 0) bands of $N_2{}^{16}O^+$ and $N_2{}^{18}O^+$ photographed under high resolution are shown in figure 2, plate 4, and the rotational branches and their assignments in $N_2{}^{16}O^+$ may be seen in figure 3, plate 5. Rough analysis distinguishes unambiguously the sub-bands involving $^2\Pi_{\frac{1}{2}}$ and $^2\Pi_{\frac{3}{2}}$ components of the $^2\Pi$ state through an appreciable Λ doubling in the $^2\Pi_{\frac{1}{2}}$-component; but although the detailed structure around the band origins makes it possible in principle to establish whether the $^2\Pi$ state is the lower or upper state in the transition, the crowding of lines obscures a clear-cut decision. Both states involved in the transition are, however, observed also as limits of Rydberg series (Tanaka *et al.* 1960) which show clearly that the $^2\Pi$ state is the

ground state of the ion, as expected from electron configurations. It is therefore inverted. Rotational analysis by itself cannot distinguish between $^2\Sigma^+$–$^2\Pi$ and $^2\Sigma^-$–$^2\Pi$ transitions even in principle (see, for example, Callomon & Morgan 1965), the parities being linked to the signs of spin-splitting and Λ doubling constants. A $^2\Sigma^-$–$^2\Pi$ transition may, however, be excluded as follows. As the two states in the transition appear with comparable strengths in both Rydberg series and photoelectron spectra, they can arise from closed-shell N_2O by the excitation in each case of one electron only. A $^2\Sigma^-$ state can, however, come only from configurations of the type $\ldots\sigma\pi^2$ or $\sigma\pi\pi$.

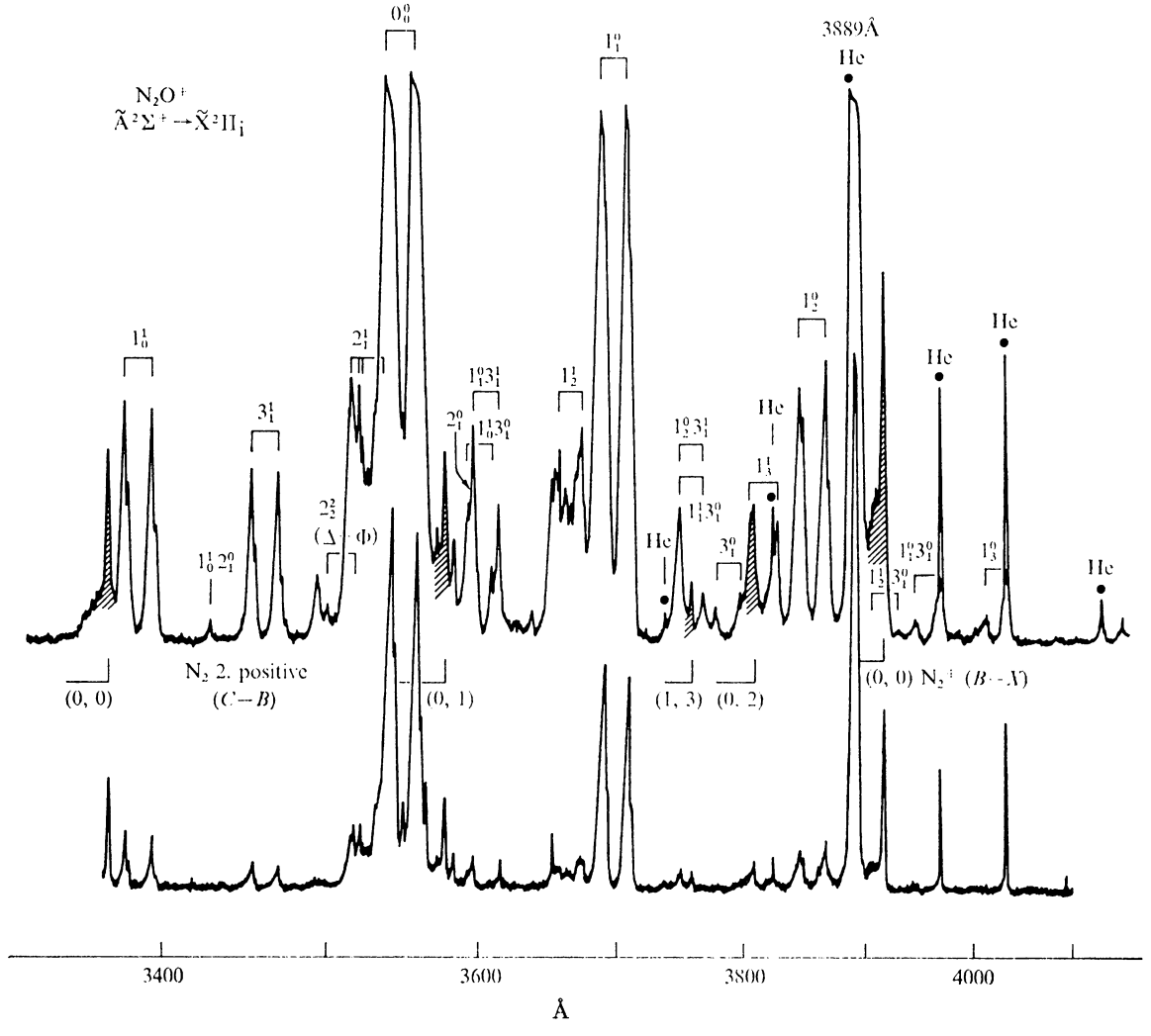

FIGURE 1. Microdensitometer traces of the emission from a hollow cathode in flowing N_2O:He premixed *ca.* 1:1000 Hilger medium quartz spectrograph; Ilford R30 plates; current 10 mA; exposures 2 and 4 s.

The principal bands in the spectrum are therefore $^2\Sigma^+$–$^2\Pi_1(a)$. The $F_2''(J)$ levels belong to $^2\Pi_{\frac{1}{2}}$ and are seen in the long-wave member of a pair of sub-bands. Wavelengths of observed band heads are collected in an Appendix together with frequencies ν_0 of band centres corresponding to the hypothetical levels $J = 0$, where known. Frequences of the rotational lines of all measured bands may be found in a thesis (Creutzberg 1964).

(*a*) *Rotational analysis*

The quality of the rotational structure observed varied widely from band to band, depending on the degree of overlapping by other bands, or branches by other branches within the same band. To obtain good constants depended therefore more on the selection of bands and branches to be analysed than their number, and some of the lesser constants could not be determined very well. The constants were obtained by standard methods from combination differences and sums. The 0–0, 1_0^1 and 1_1^0 bands of both isotopes and the 3_1^1 band of the normal species were extensively analysed. They are all of type $^2\Sigma$–$^2\Pi$, and could be fitted to expressions based on near case (*a*) or case (*b*) term values:

$$^2\Sigma^+\colon F_{1,2}(N)_v = B_v N(N+1) - D_v N(N+1)^2 + \phi(N), \tag{1}$$

where $\phi(N) = +\frac{1}{2}\gamma N$ for F_1, $J = (N+\frac{1}{2})$, and $\phi(N) = -\frac{1}{2}\gamma(N+1)$ for F_2, $J = (N-\frac{1}{2})$. Excitation of the degenerate bending vibration introduces additional terms of the type $\pm\frac{1}{2}q_2^l N(N+1)$ giving the l doubling components different effective rotational constants

$$B_{\mathrm{eff},v} = (B_v \pm \tfrac{1}{2}q_2^l).$$

For $^2\Pi_1$ near case (*a*) expansion of the Hill–Van Vleck formula (Mulliken 1930) gives

$$^2\Pi_1\colon F_{1,2}(J)_v = \pm\tfrac{1}{2}A_v - \tfrac{3}{4}B_v \mp B_v(1 \pm 3B_v/4A_v) + B_{\mathrm{eff},1,2,v}J(J+1) - D_{\mathrm{eff},1,2,v}J^2(J+1)^2 \pm \tfrac{1}{2}\phi(J), \tag{2}$$

where A_v is the (signed) spin-orbit coupling constant; $B_{\mathrm{eff},1,2}$ are effective rotational constants related to the constants $B_{1,2,v}$ by the Mulliken correction

$$B_{\mathrm{eff},1,2,v} = B_{1,2,v}(1 \pm B_v/A_v) \tag{3}$$

and $B_{1,2,v}$ are related to the true inertial constant B_v by the James correction (1964)

$$B_{1,2,v} = B_v \pm 2A_{vJ}, \tag{4}$$

which arises from the dependence of the spin-orbit coupling constant on centrifugal distortion. The Λ doubling $\phi(J)$ can be reduced to the form

$$^2\Pi_{\frac{1}{2}},\ F_2\colon \Delta F_{c-d}(J) = p(J+\tfrac{1}{2}) - s(J+\tfrac{1}{2})^3, \tag{5a}$$

$$^2\Pi_{\frac{3}{2}},\ F_1\colon \Delta F_{c-d}(J) = \quad -s(J+\tfrac{1}{2})^3, \tag{5b}$$

where $s = (2q/Y)$; $Y = A/B$, the case (*a*)–(*b*) uncoupling parameter; and p and q are constants. All these formulae neglect terms other than the leading ones in powers of $J(J+1)$ or $(J+\frac{1}{2})$, so that the minor constants D, q obtained by fitting the data to these formulae may not be very close to the centrifugal or uncoupling constants with simple physical significance expected from theory (in which $q = p/2Y$).

Other bands involving stretching vibrations were only partially analysed. In almost all cases the transition had one state in common with those completely analysed, so that to determine the band-origins, for vibrational analysis, a relatively crude estimate of $(B'-B'')$ and a few line frequencies in a branch or even band head sufficed. Good enough values of $(B'-B'')$ could be obtained from the separations of heads in the double headed sub-bands which turn at values of J at which contributions from D, p and q could be neglected.

In a few further bands the $^2\Sigma^{(+)}$ component of the $^2\Pi$, $v_2 = 1$ vibronic manifold was resolved.

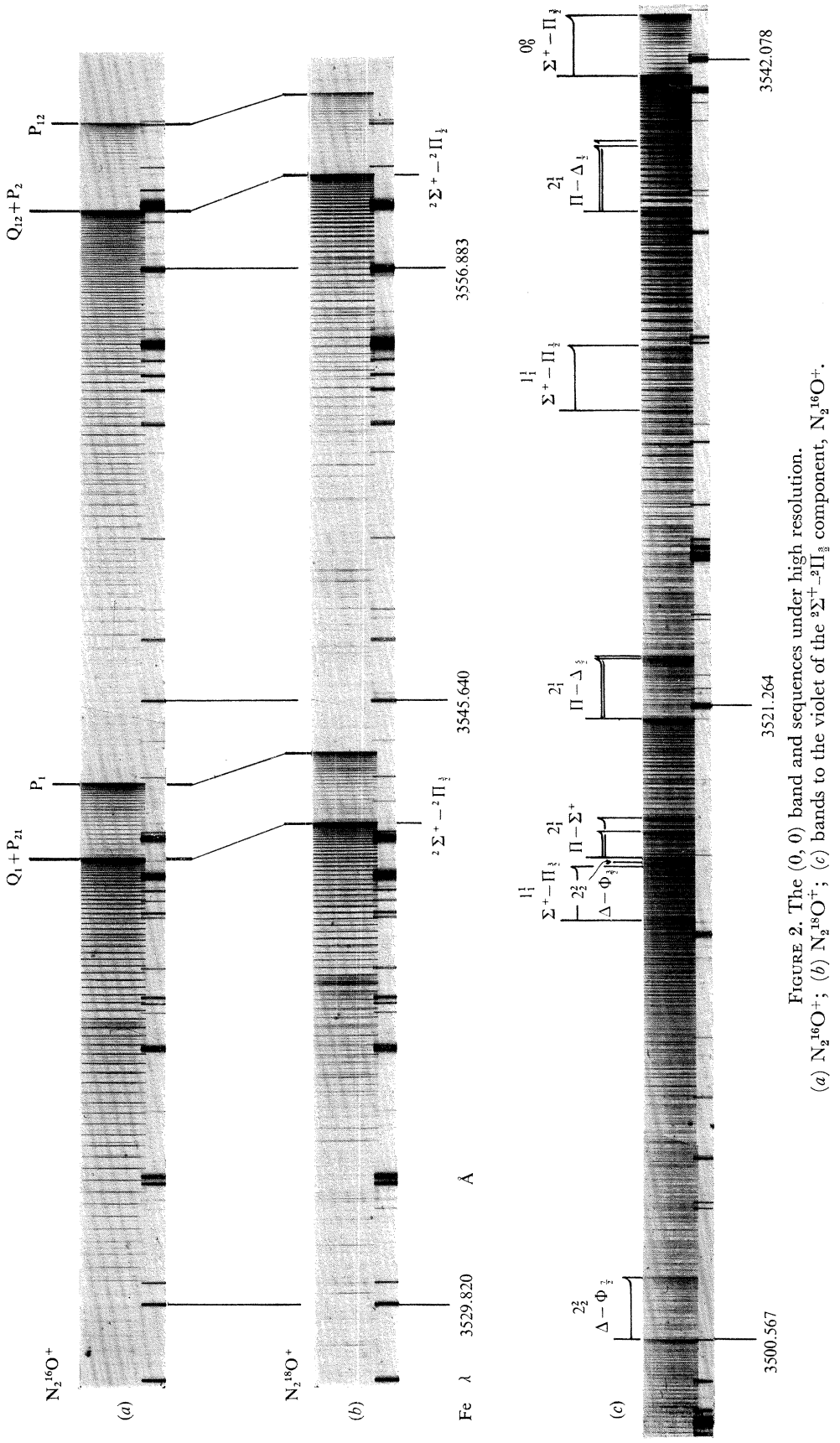

FIGURE 2. The (0, 0) band and sequences under high resolution.
(*a*) $N_2^{16}O^+$; (*b*) $N_2^{18}O^+$; (*c*) bands to the violet of the $^2\Sigma^+-^2\Pi_{\frac{3}{2}}$ component, $N_2^{16}O^+$.

(*Facing p.* 162)

PHILOSOPHICAL TRANSACTIONS OF THE ROYAL SOCIETY A MATHEMATICAL, PHYSICAL & ENGINEERING SCIENCES

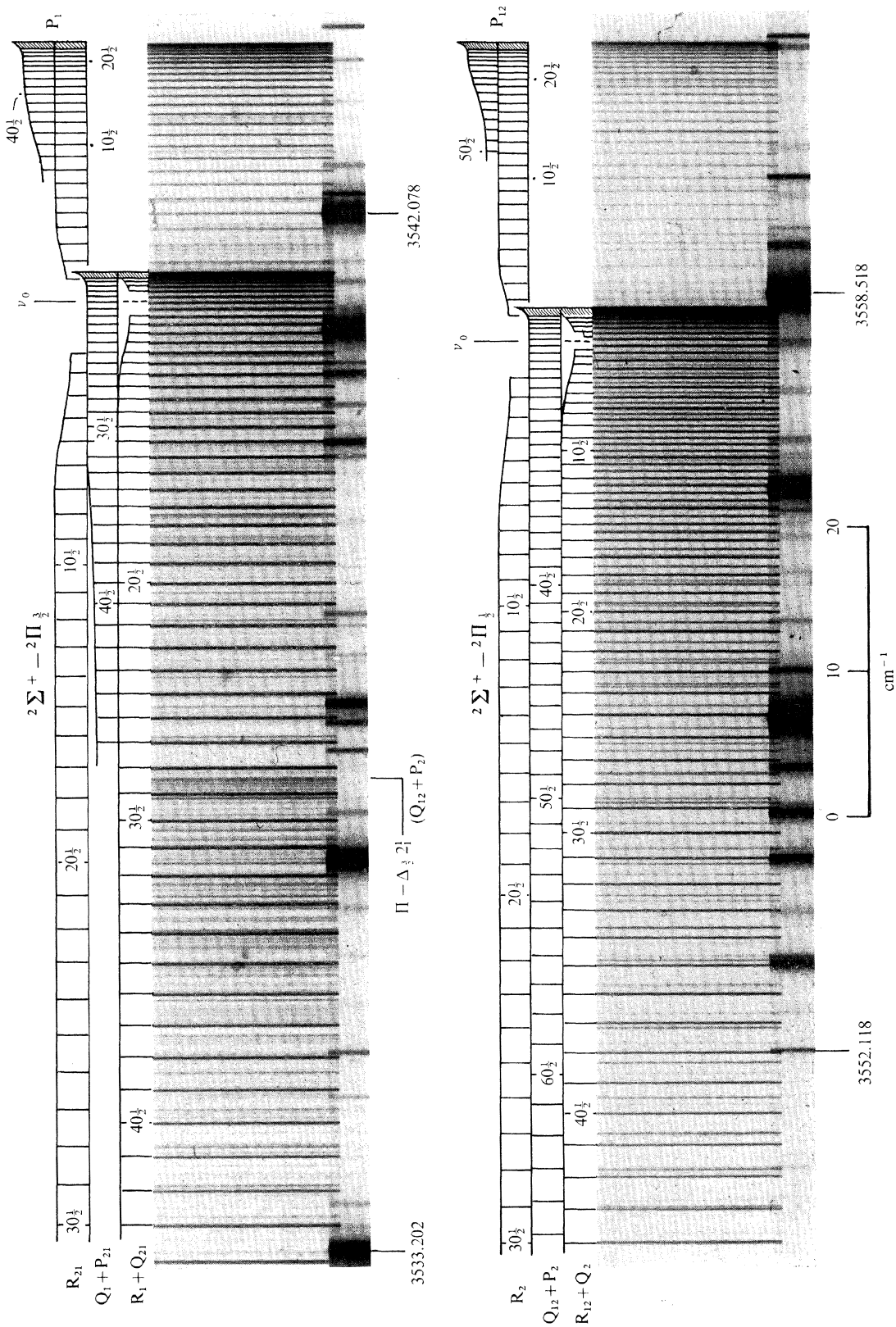

FIGURE 3. The (0, 0) band of $N_2^{16}O^+$, showing the rotational assignments of branches.

PHILOSOPHICAL TRANSACTIONS OF THE ROYAL SOCIETY A MATHEMATICAL, PHYSICAL & ENGINEERING SCIENCES

For the present magnitudes of spin-orbit and Renner couplings such vibronic $^2\Sigma$-states behave like pure electronic case (b) states, described above, except that the doublet splitting constant γ is very large, of the order of B, and does not have a simple spin-rotation interpretation; and the B values are again effective constants containing spin-vibronic contributions (see Herzberg 1966, p. 75, after Hougen).

The expressions for the energy levels of the excited $^2\Sigma$ state being the simplest, the analysis concentrated primarily on determining the rotational constants B and D of this state. Those of the ground state were then obtained relative to those of the excited state, making use of the fact that differences of constants, $(B'-B'')$ and $(D'-D'')$ can be obtained independently from line combinations between branches in a band with absolute precisions that exceed those of the constants themselves by at least an order of magnitude. The experimental values and constants thus obtained are given in tables 2 and 4 for the four bands analysed in detail, and the less precise constants for some other bands, based essentially also on differences $(B'-B'')$ obtained from branch head separations, are given in table 3.

The Λ doubling constants for the ground state cannot be obtained from simple combination relations but require pairs of combination differences (see, for example, Callomon & Morgan 1965) and hence incorporate the scatter of lines in four branches. They are therefore not very precise. The values are in table 4. The spin splitting (ρ doubling) constant γ in the excited $^2\Sigma$ state is very small. It should appear immediately in the spectra as a splitting of the narrowly

TABLE 2. PRINCIPAL ROTATIONAL CONSTANTS B FROM ROTATIONAL ANALYSIS/cm^{-1}

	band	constant	$N_2{}^{16}O^+$		$N_2{}^{18}O^+$	
1	1_0^1	B'_{100}	0.43098	(6)	0.40724	(6)
2	1_0^1	B'_{000}†	0.43300	(6)	0.40909	(7)
3	0–0	B'_{000}	0.43300	(5)	0.40909	(6)
4	1_1^0	B'_{000}	0.43296	(6)	0.40908	(6)
5	3_1^1	B'_{001}	0.42952	(10)	—	
6	1_1^2	B'_{200}	0.4290	(5)	—	
7	$2_1^1K_2^1$	B'_{010}	0.4322	(5)	—	
8	0–0	$(B'-B''_1)$	0.022739	(30)	0.021571	(3)
9	1_0^1	$(B'-B''_1)$	0.020717	(3)	0.019707	(10)
10	0–0	$B''_{000,\,\mathrm{eff}}(F_1)$	0.41026	(8)	0.38752	(6)
11	1_0^1	$B''_{000,\,\mathrm{eff}}(F_1)$	0.41026	(6)	0.38753	(6)
12	0–0	$(B'-B''_2)$	0.020097	(3)	0.019216	(3)
13	1_0^1	$(B'-B''_2)$	0.018081	(3)	0.017376	(10)
14	0–0	$B''_{000,\,\mathrm{eff}}(F_2)$	0.41290	(5)	0.38987	(7)
15	1_0^1	$B''_{000,\,\mathrm{eff}}(F_2)$	0.41290	(6)	0.38986	(7)
16	1_1^0	$(B'-B''_1)$	0.025500	(30)‡	—	
17	1_1^0	$B''_{100,\,\mathrm{eff}}(F_1)$	0.40746	(9)	—	
18	1_1^0	$(B'-B''_2)$	0.023603	(5)	0.022460	(5)
19	1_1^0	$B''_{100,\,\mathrm{eff}}(F_2)$	0.40936	(7)	0.38663	(6)
20	3_1^1	$(B'-B''_1)$	0.021925	(10)§	—	
21	3_1^1	$B''_{001,\,\mathrm{eff}}(F_1)$	0.40760	(11)	—	
22	3_1^1	$(B'-B''_2)$	0.019291	(10)	—	
23	3_1^1	$B''_{001,\,\mathrm{eff}}(F_2)$	0.41023	(11)	—	

Figures in parentheses are standard errors in the last digits quoted.

Data in rows 1, 3–9, 12–13, 16, 18, 20, 22 are independent. The remaining constants are derived from them.

Constants in rows 1, 3 and 4 are from $^2\Sigma$–$^2\Pi_{\frac{1}{2}}$ sub-bands only, being the best resolved. Row 5: combined from both sub-bands. Rows 6–7: partial analyses.

F_1, F_2 refer to $^2\Pi_{\frac{3}{2}}$ and $^2\Pi_{\frac{1}{2}}$ components of $^2\Pi$.

† From B'_{100} and α'_{100}, obtained from rows 8 and 9 or 12 and 13.

‡ Heavily perturbed; from lines $J \leqslant 20\frac{1}{2}$.

§ Perturbed; from lines $J \geqslant 28\frac{1}{2}$.

TABLE 3. PRINCIPAL ROTATIONAL CONSTANTS B''_v of $N_2{}^{16}O^+$, GROUND STATE, FROM BAND-HEAD SEPARATIONS/cm^{-1}

constants	F_1, $^2\Pi_{\frac{3}{2}}$	F_2, $^2\Pi_{\frac{1}{2}}$
$B''_{200,\,\mathrm{eff}}$	0.4099	0.4057
$B''_{300,\,\mathrm{eff}}$	0.3995	0.4020
$B''_{400,\,\mathrm{eff}}$	0.3959	0.3984
$B''_{101,\,\mathrm{eff}}$	0.4049	0.4073
$B''_{201,\,\mathrm{eff}}$	0.4022	0.4042
$B''_{010}(^2\Delta)$	0.4101	0.4128
$B''_{010}(^2\Sigma^{(+)})$	0.4136	

Uncertainties estimated to be ± 0.0005 cm $^{-1}$.

TABLE 4. MINOR ROTATIONAL CONSTANTS/cm^{-1}

band	constant	$N_2{}^{16}O^+$		$N_2{}^{18}O^+$	
1^1_0	$10^7 D'_{100}$	1.70	(0.10)	1.50	(0.15)
0–0	$10^7 D'_{000}$	1.78	(0.10)	1.53	(0.10)
1^0_1	$10^7 D'_{000}$	1.78	(0.10)	1.82	(0.15)
3^1_1	$10^7 D'_{001}$	1.60	(0.30)	—	
0–0	$10^7(D'-D''_1)$	—		−0.11	(0.01)
1^1_0	$10^7(D'-D''_1)$	−0.037	(0.005)	−0.11	(0.01)
0–0	$10^7 D''_{000,\,\mathrm{eff}}(F_1)$	—		1.64	(0.11)
1^1_0	$10^7 D''_{000,\,\mathrm{eff}}(F_1)$	1.74	(0.11)	1.61	(0.16)
0–0	$10^7(D'-D''_2)$	−0.37	(0.20)	−0.37	(0.01)
1^1_0	$10^7(D'-D''_2)$	−0.337	(0.010)	−0.40	(0.10)
0–0	$10^7 D''_{000,\,\mathrm{eff}}(F_2)$	2.15	(0.30)	1.90	(0.11)
1^1_0	$10^7 D''_{000,\,\mathrm{eff}}(F_2)$	2.04	(0.11)	1.90	(0.25)
0–0	$10^3 p$	1.7	(0.1)	1.1	(0.1)
1^1_0	$10^3 p$	1.9	(0.1)	1.4	(0.2)
0–0	$10^5 q$ (F_1)	—		—	—
1^1_0	$10^5 q$ (F_1)	2.3	(1.0)	1.2	(1.0)
0–0	$10^5 q$ (F_2)	7.4	(0.5)	1.5	(1.0)
1^1_0	$10^5 q$ (F_2)	11	(5)	2.9	(0.3)
	level $(100)''$				
1^0_1	$10^7 D_{\mathrm{eff}}$ (F_1)	—		—	
	$10^7 D_{\mathrm{eff}}$ (F_2)	2.23	(0.13)	2.15	(0.18)
	$10^3 p$ (F_2)	1.45	(0.20)	1.8	(0.2)
	$10^5 q$ (F_2)	5.5	(2.0)	4.7	(2.0)
	level $(001)''$				
3^1_1	$10^7 D_{\mathrm{eff}}$ (F_1)	1.53	(0.31)	—	
	$10^7 D_{\mathrm{eff}}$ (F_2)	1.87	(0.36)	—	
	$10^3 p$ (F_2)†	1.30	(0.20)	—	
	$10^5 q$ (F_1)	5.9	(2.0)	—	
	$10^5 q$ (F_2)	7.2	(1.0)	—	
	level $(010)''$ $^2\Sigma^{(+)}$				
$1^1_0 2^0_1$, 2^0_1	$10^3\gamma(\Sigma^{(+)})$	176‡	(20)	—	
	level $(000)'$				
1^0_1	$10^3\gamma$	$\leqslant 1.5$§			
	level $(010)'$				
$2^1_1 K^1_2$	$10^3 q'_2$	0.77‖	(0.10)		

† Level ν''_3 of $^2\Pi_{\frac{3}{2}}$ is perturbed and shows a linear splitting of the Kramers degeneracy given by an effective Λ-doubling constant $p(F_1) = 9.3 \pm 0.4 \times 10^{-3}$ cm^{-1}.

‡ From separation of P_1–P_2 heads. Calculated value 168 (see text).

§ Errors coupled to those in D, p and q of $^2\Pi_{\frac{1}{2}}$ (see text).

‖ From splitting of P_1 head.

spaced pairs of branches (Q_{12}, P_2), (R_{12}, Q_2), (Q_1, P_{21}) and (R_1, Q_{21}), but apart from a slight broadening of lines at high J no effects of γ are apparent and these branches are never individually resolved. The only sources of evidence are then the widely spaced P and R branches, which were combined in the best resolved sub-band, $^2\Sigma - {}^2\Pi_{\frac{1}{2}}$ of 1_1^0, according to the relation

$$[P_{12}(J+2) - R_2(J-1)] + [F''_{2d}(J+2) - F''_{2c}(J-1)] = \gamma(J+1)$$

the lower state term values being calculated from the constants obtained from the rest of the analysis. The value of γ obtained in this way is $+0.0006 \pm 0.0003$ cm^{-1}, but the absolute uncertainty is probably considerably greater and hard to estimate because it contains contributions from all the constants used to calculate the term values of F''_2.

The value of γ in the $^2\Sigma^{(+)}$ level of the $v''_2 = 1$ manifold in the ground state came from P_2–P_1 branch head separations in the observed parallel bands. It may be compared with a value to be expected theoretically (Herzberg 1966, p. 77, after Hougen) from the spin-orbit and Renner coupling parameters, derived below, of 200×10^{-3} cm^{-1}. The difference may just be significant, and is comparable to that found in the molecule NCO (Dixon 1960: $10^3\gamma$ (obs.) = 118 cm^{-1}; $10^3\gamma$ (calc.) = 78 cm^{-1}).

TABLE 5. VARIATION OF ROTATIONAL CONSTANTS B WITH VIBRATIONAL STATE

level, $(v_1 v_2 v_3)$		$10^3(B_v - B_0)$/cm^{-1} $N_2{}^{16}O$		$N_2{}^{18}O$	
		excited state, $^2\Sigma^+$			
(100)		−2.019	(5)	−1.852	(13)
(200)		−4.0	(5)	—	
(101)		−0.8	(5)	—	
(001)		−3.48	(15)	—	
		ground state, $^2\Pi_{\frac{3}{2}}(F_1)$, $^2\Pi_{\frac{1}{2}}(F_2)$			
(100)	F_1	−2.761	(60)	—	
	F_2	−3.506	(8)	−3.244	(8)
(200)	F_1	−0.4	(5)	—	
	F_2	−7.2	(5)	—	
(300)	F_1	−10.8	(5)	—	
	F_2	−10.9	(5)	—	
(400)	F_1	−14.4	(5)	—	
	F_2	−14.5	(5)	—	
(010)	$^2\Delta_{\frac{5}{2}}$	−0.2	(5)	—	
	$^2\Delta_{\frac{3}{2}}$	−0.1	(5)	—	
	$^2\Sigma^{(+)}_{\frac{1}{2}}$	+1.8†	(5)	—	
(001)	F_1	−2.66	(16)	—	
	F_2	−2.67	(16)	—	
(101)	F_1 (obs)	−5.4	(5)	—	
	(calc)	(−6.2)	(2)		
	F_2 (obs)	−5.6	(5)	—	
	(calc)	(−6.2)	(2)		
(201)	F_1 (obs)	−8.1	(5)	—	
	(calc)	(−9.7)	(2)		
	F_2 (obs)	−8.7	(5)	—	
	(calc)	(−9.7)	(2)		

† B_{eff}–B_{000}, the mean of the zero point B_{eff} in the two spin components, and corrected for a small spin-orbit-Renner factor (see Herzberg 1966, p. 77, equation I, 92) of $0.2_2 \times 10^{-3}$ cm^{-1}.

PHILOSOPHICAL TRANSACTIONS OF THE ROYAL SOCIETY A MATHEMATICAL, PHYSICAL & ENGINEERING SCIENCES

TABLE 6. MOLECULAR ROTATIONAL CONSTANTS FOR N_2O^+/cm^{-1}

constant	$N_2{}^{16}O$		$N_2{}^{18}O^+$	
	excited state, $\tilde{A}^2\Sigma^+$			
B_{000}	0.43300	(4)	0.40909	(4)
$10^7 D_{000}$	1.75	(8)	1.60	(10)
$10^3\alpha_1$	2.02	(1)	1.85	(1)
$10^3\alpha_2$	0.8	(5)	—	
$10^3\alpha_3$	3.48	(15)	—	
$10^3\gamma$	$\leqslant 1.5$		—	
$10^3 q_2^l$	0.8	(1)	—	
B_e	0.4365	(6)	—	
	ground state, $\tilde{X}^2\Pi$			
B_{000}	0.41158	(5)	0.38869	(5)
$10^7 D_{000}$	1.90	(15)	1.76	(15)
$10^3\alpha_1$	3.51	(1)	3.24	(1)
$10^3\alpha_2$	0.85	(5)	—	
$10^3\alpha_3$	2.66	(16)	—	
$10^3 p$	1.8	(1)	1.2	(1)
$10^5 q(F_1)$	2.3	(1)	1.2	(1)
$10^5 q(F_2)$	7.4	(5)	2.9	(3)
B_e	0.4138	(5)	—	
$10^3[B_{000,\,\mathrm{eff}}(F_2) - B_{000,\,\mathrm{eff}}(F_1)$	2.636	(6)	2.345	(15)
$10^3[B_{000}(F_2) - B_{000}(F_1)]$	0.076	(6)	0.062	(15)
$10^5 A_J$	−3.8	(3)	−3.1	(8)

Values of α, and hence B_e, not corrected for possible anharmonic resonances.

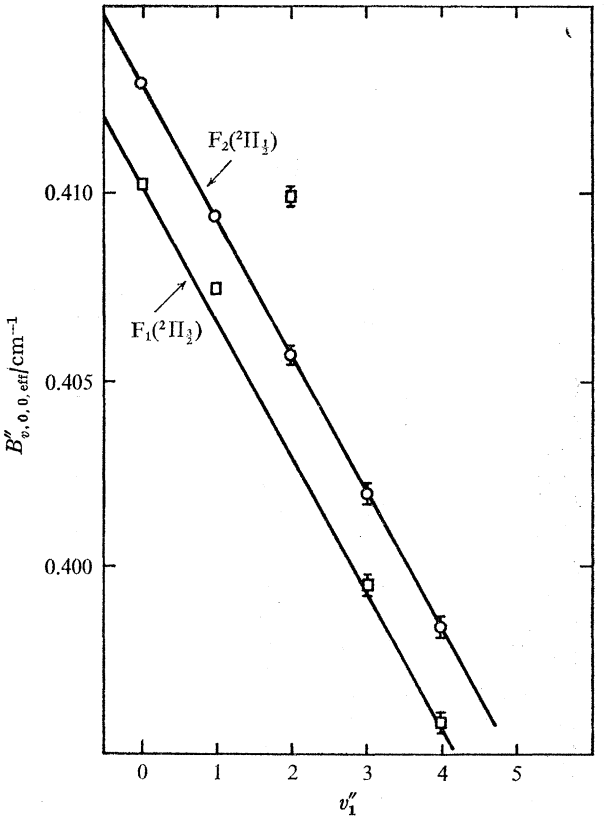

FIGURE 4. Plot of $B''_{v,\,0,\,0,\,\mathrm{eff}}$ against $(v_1 + \frac{1}{2})$ for the two spin-components of the $\tilde{X}\,^2\Pi$ state, showing the irregularities due to perturbations in $^2\Pi_{\frac{3}{2}}$.

PHILOSOPHICAL TRANSACTIONS OF THE ROYAL SOCIETY A MATHEMATICAL, PHYSICAL & ENGINEERING SCIENCES

There is limited information on the variation of B_v with v. Values of $(B_v - B_0)$ are listed in table 5, based on the primary data in tables 2–4. They are used to derive a set of α_v values given in table 6. In the excited state the only vibration observed in excitation of more than one quantum is ν_1, and $(B'_{200} - B'_{000})$ is exactly twice $(B'_{100} - B'_{000})$ within the rather poor experimental precision. There is therefore no way of telling whether the Fermi resonance to be expected between ν'_1 (1345 cm^{-1}) and $2\nu'_2$ ($2 \times 614 = 1228$ cm^{-1}) has an appreciable effect on the rotational constants or not, and α's are simply taken to be $B'_{v_1=1} - B'_{000}$. In the ground state ν_1 can be followed up to four quanta and the variation of $B''_{\mathrm{eff},v}$ in both spin components is shown in figure 4. The points for the F_2 component all lie well on the straight line drawn with gradient given by the two precisely determined points B_{000} and B_{100}, but those for the F_1 component show a considerable scatter reflecting extensive perturbations which are discussed further below. At higher v they return to the straight line through $v = 0$ with the same gradient as in F_2, which is thus taken to be the value of α''_1 for both components. Fermi resonance, if present, does not appear to be strong. Only one quantum of ν''_3 was observed and while the rotational structure in 3^1_1 directly shows this to be strongly perturbed in F_1 (see below), vibrational analysis suggests that the F_2 component may also be affected. Nevertheless both components give roughly the same value for $(B''_{001} - B''_{000})$ which has therefore to be taken as the only available guide to α''_3. The values of α''_1 and α''_3 thus obtained then reproduce the values of B for two other combination levels probably as well as can be expected. The value of α''_2 adopted is the mean of two estimates based on the $^2\Sigma^{(+)}$ and $^2\Delta_{\frac{3}{2}}(F_2)$ components of the $v''_2 = 1$ manifold.

Even less can be said about the Λ doubling constants. The isotopic ratio of p is much greater than expected, which is that for B; and the q values, which should be the same for F_1 and F_2 components, are an order of magnitude greater than the p/Y that simple theory predicts. Variation of D with v is hardly significant in either state, and in the ground state quite overshadowed by what appears to be a small but genuine difference in D_{eff} between spin components of $0.3 \pm 0.2 \times 10^{-7}$ cm^{-1}. It may be that the discrepancies in q and D in the ground state are linked in experimental uncertainty, for calculation of D from force fields (see below), while giving values that agree well with the experimentally observed ones for the excited state, suggest that the experimental values of the ground state are a little too small.

Applying the Mulliken Λ uncoupling corrections to the effective ground state B values in the two spin components leaves a residual difference which may be ascribed to the centrifugal spin-orbit James correction (assuming $\Delta B_{000} \approx \Delta B_e$). If this is correct then the derivative of the spin-orbit coupling constant with respect to nuclear stretching displacements,

$$\sum_{i=1,3} (\partial |A| / \partial Q_i)$$

appears to be positive (for discussion, see Anderson & Callomon 1973).

All the rotational constants finally adopted are collected in table 6.

(*b*) *Electronic orbital and spin terms*

Band centres of rotationally analysed sub-bands are given in table 7. They are the term values of the hypothetical levels $J = 0$, from which the purely orbital electronic zero point transition energy T_{00} and effective spin-orbit coupling constant $A_{\mathrm{eff},0}$ can be obtained through the Hill–Van Vleck equation, (2), above. These constants are also in table 7.

This definition of electronic energy differs by $+\frac{1}{2}B$ from that given by the pure case (a) symmetric-top model, quoted by Herzberg (1950), equation V. 12. Note also that, although it takes as origin the true vibrational zero point of the $^2\Pi$ ground state corrected for first order spin-orbit coupling, and is in that sense experimentally observable, the zero point energy includes slightly less than the whole quantum ω_2 of bending vibration expected for the simple two-dimensional oscillator, by an amount $\frac{1}{4}\epsilon^2\omega_2$ arising through Renner–Teller coupling. Although thus a wholly theoretical quantity, this small correction must be taken into account in the analysis and computation of higher quanta of the bending vibration, discussed below. The various small corrections linking rospinvibronic origins ($J = 0$), rotationless spin-vibronic terms ($N = 0$) and pure vibrational terms may be seen in figure 7.

TABLE 7. BAND ORIGINS (ν_0, $J = 0$), ELECTRONIC AND SPIN-ORBIT COUPLING CONSTANTS/cm^{-1}

band	component	$N_2{}^{16}O^+$		$N_2{}^{18}O^+$	
0–0	$^2\Sigma$–$^2\Pi_{\frac{3}{2}}(F_1)$	28229.941	(10)	28222.516	(10)
	$^2\Sigma$–$^2\Pi_{\frac{1}{2}}(F_2)$	28096.757	(3)	28089.395	(3)
	$\Delta\nu_{2-1}$	133.184	(13)	133.121	(13)
1_0^1	(F_1)	29575.460	(3)	29527.131	(5)
	(F_2)	29442.271	(3)	29393.991	(10)
	$\Delta\nu_{2-1}$	133.189	(6)	133.140	(15)
1_1^0	(F_1)	27103.435	(20)	—	
	(F_2)	26970.337	(3)	27001.098	(3)
	$\Delta\nu_{2-1}$	133.098	(23)	—	
3_1^1	(F_1)	28943.853	(10)	—	
	(F_2)	28812.641	(5)	—	
	$\Delta\nu_{2-1}$	131.212	(15)	—	
	T_{00}	28163.040	(13)	28155.664	(13)
	$A_{\text{eff}(0,1)}$	−132.359	(13)	−132.342	(13)
	A_0	−133.597	(13)	−133.579	(13)
	$Y_0 = A_0/B_0$	−324.59	(7)	−343.66	(7)

Constants from detailed rotational analysis. Band centres of other bands estimated from head centre separations are given in the Appendix.

The A_{eff} obtained as the separation of the rotationless spin-vibronic components of the $^2\Pi$ ground state is also slightly less than the pure case (a) spin-orbit coupling constant A_0. It is $A_{\text{eff},K} = A_{\text{eff},1}$ (Herzberg 1966, equation I. 98):

$$A_{\text{eff},1} = A_0[1 - \tfrac{1}{4}\epsilon^2], \tag{6}$$

where ϵ is the Renner coupling parameter. Hence A_0, also given in table 7. The values for the two isotopes are identical within their uncertainties.

The doublet splitting of the ground state appears to vary somewhat with the vibration excited (see table 7). Nothing can be deduced from this however about the vibrational dependence of the spin-orbit coupling constant, for its effects, if any, are inseparable from those of differential vibrational perturbations in the doublet components, such as Fermi or other anharmonic resonances, which are unlikely to be negligible in any of the excited levels observed.

(c) *Vibrational analysis: stretching vibrations* ν_1, ν_3

The observed levels involving the stretching vibrations are shown diagrammatically in figure 5. The vibrational term values were obtained as combination differences using mainly frequencies of band centres, given in the appendix, obtained from the frequencies of band heads and estimates of head centre separations from rough rotational constants. How well this works may be seen in an example in table 8. Data for $N_2{}^{18}O^+$ are much less extensive than for $N_2{}^{16}O^+$ because only the stronger bands were photographed under high resolution. Values of ν_3' and $(\nu_1''+\nu_3'')$ are most precisely accessible in this case through double differences, e.g. $\nu_3' = (1_0^1 - 0) + (3_1^1 - 1_0^1 3_1^0)$.

As only ν_1' was observed in more than two quanta little can be said about anharmonicities. The variation of $G_0''(v_1)$ with v_1 is shown in figure 6. The points for the upper doublet component (F_2, $^2\Pi_{\frac{1}{2}}$) of the ground state fall fairly closely on a straight line, but those for the lower component scatter, reflecting perturbations already seen in the analogous plots for the rotational constant B in figure 4. These perturbations are discussed again below.

In the excited state a Fermi resonance is expected between ν_1' and $2\nu_2'$ but as $2\nu_2'$ was not observed and $(B'_{200}-B'_{000})$ was twice $(B'_{100}-B'_{000})$ within experimental error, nothing can be

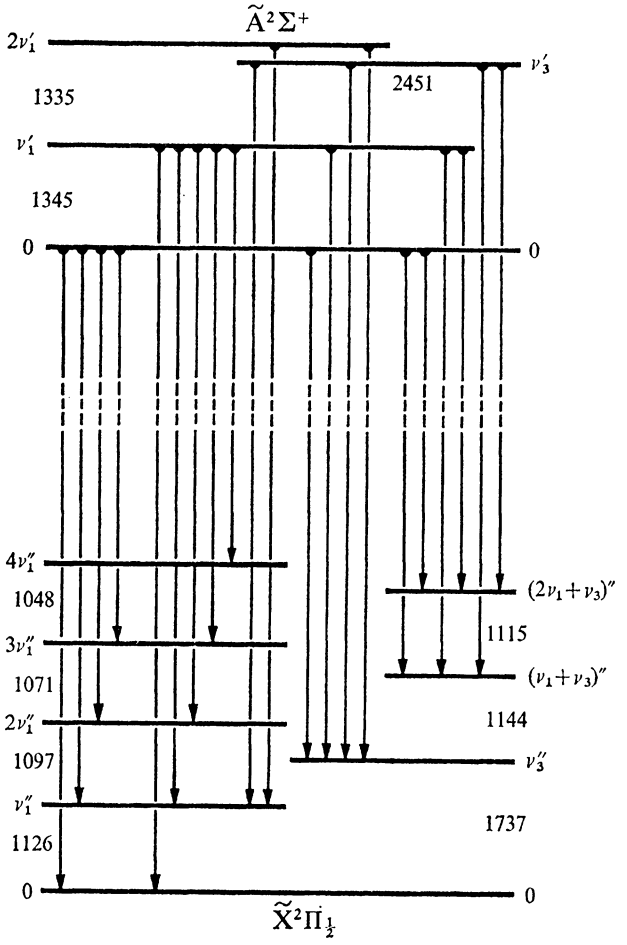

FIGURE 5. Levels and transitions observed involving the stretching vibrations, ν_1 and ν_3. Only the unperturbed $^2\Pi_{\frac{1}{2}}$ component of the lower state is shown.

TABLE 8. VIBRATIONAL COMBINATION-DIFFERENCES ISOLATING QUANTA OF THE STRETCHING-VIBRATION ν_1

bands, level ν_1'	$N_2{}^{16}O^+$	$N_2{}^{18}O^+$
	excited state	
1_0^1–0 (F_1'')	1345.52	1304.61
(F_2'')	1345.51	1304.59
1_1^1–1_1^0 (F_1'')	1345.5	—
(F_2'')	1345.5	—
1_2^1–1_2^0 (F_1'')	1345.6	1302
(F_2'')	1345.4	1303
1_3^1–1_3^0 (F_1'')	1345.5	1305
(F_2'')	1345.6	1305
1_4^1–1_4^0 (F_1'')	1345.4	—
(F_2'')	1345.5	—
$1_0^1 3_1^0$–3_1^0 (F_1'')	1345.7	—
(F_2'')	1345.6	—
$1_1^1 3_1^0$–$1_1^0 3_1^0$ (F_1'')	1345.5	—
(F_2'')	1345.4	1305
$1_2^1 3_1^0$–$1_2^0 3_1^0$ (F_1'')	1345.3	—
(F_2'')	1345.5	—
$1_0^1 2_1^0$–2_1^0 ($\Sigma^{(+)''}$)	1345.6	1304.5

Frequencies to two decimal places from bands rotationally analysed; to one decimal, from band heads photographed under high resolution with estimates of head centre separations; to nearest whole number, from band heads under low resolution.

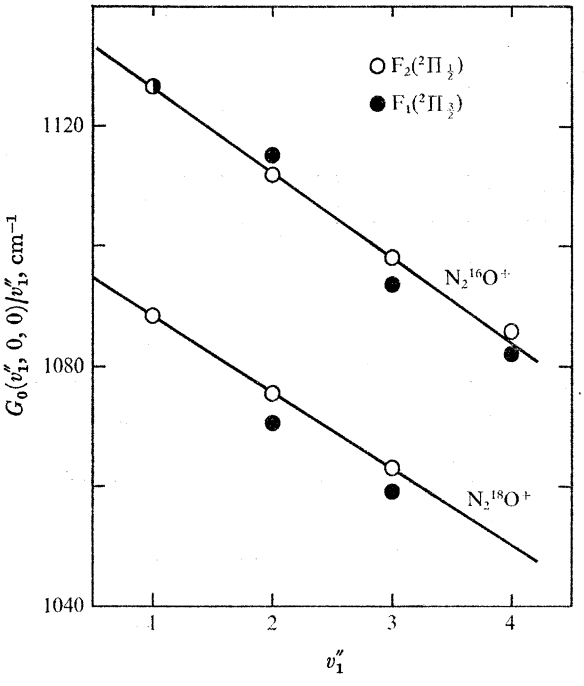

FIGURE 6. The dependence of successive quanta of ν_1'' on vibrational quantum number v_1''. In the first order anharmonic approximation $G_0(100) = \omega_1 - 2\omega_1 x_1$, and the gradients of the lines are $\omega_1 x_1$. Note the irregularities in the F_1 component ($^2\Pi_{\frac{3}{2}}$) due to perturbations.

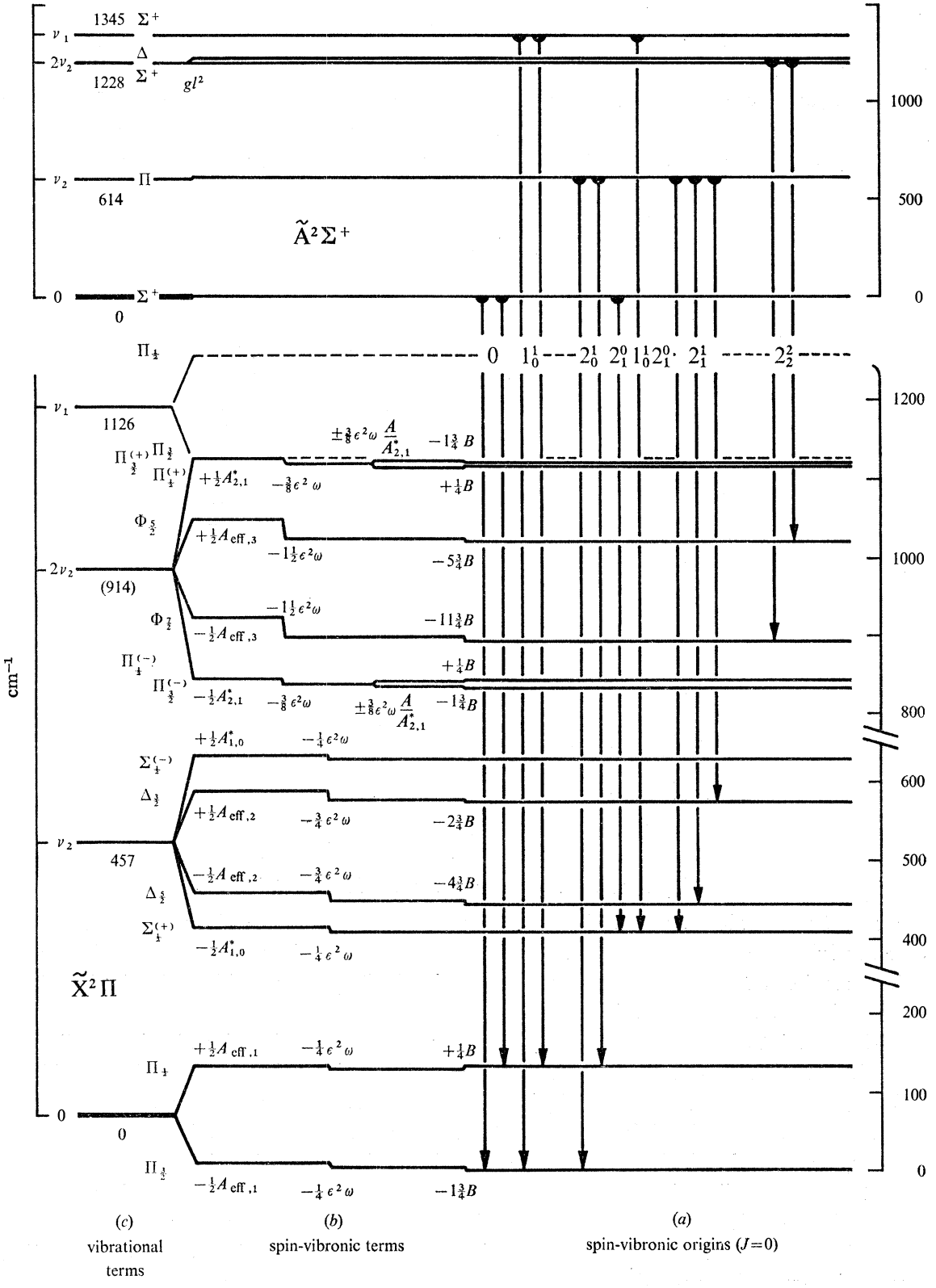

FIGURE 7. Spin-vibronic levels and observed transitions involving the bending vibration up to $v_2 = 2$. Levels v_1' and v_1'' are included, as are the transitions (0, 0) and 1^1_0, to show their positions as possible sources of perturbation and to point to the combination differences which were used in analysis. Members of a vibronic manifold drawn roughly to scale (on the right), vibrational intervals foreshortened.

PHILOSOPHICAL TRANSACTIONS OF THE ROYAL SOCIETY A MATHEMATICAL, PHYSICAL & ENGINEERING SCIENCES

said about its magnitude. It contributes an unknown amount to the variations of $G'_0(v_1 00)$ with v_1, and any attempt to interpret this in terms of an anharmonic constant x'_{11} is therefore probably meaningless.

The values adopted for the fundamental frequencies together with the constants x''_{11} from the gradients of figure 6 are included in table 11. This also includes the Teller–Redlich product rule ratio $\rho(\nu_1\nu_3)$ (Herzberg 1945, p. 231) according to which, for harmonic vibrations,

$$\rho(\nu_1\nu_3) = \nu_1^i\nu_3^i/\nu_1\nu_3 = (m_O M^i/m_O^i M)^{\frac{1}{2}},$$

m_O, M being the masses of atomic oxygen and N_2O, and superscripts i referring to the isotopically substituted species.

TABLE 9. COMBINATION-DIFFERENCES BETWEEN BAND-CENTRES ISOLATING SPIN-ROVIBRONIC ORIGINS ($J = 0$) OF LEVELS IN ν_2/cm^{-1}

bands, levels	$N_2{}^{16}O^+$	$N_2{}^{18}O^+$
excited state		
level ν'_2		
2^1_0–0 (F''_1)	614.2	—
2^1_0–0 (F''_2)	614.1	—
$2^1_1K^1_0{}^{(+)}$–$2^0_1K^0_0{}^{(+)}$	613.9	610.2
ground state†		
level ν''_2 ($v_2 = 1$)		
$K = 0$, $\Sigma^{(+)}$		
0–$2^0_1K^0_0{}^{(+)}$	412.6	411.1
1^1_0–$1^1_02^0_1K^0_0{}^{(+)}$	413.6	411.2
$2^1_0K^1_1$ (F''_1)–$2^1_1K^1_0{}^{(+)}$	412.9	—
$K = 2$, $\Delta_{\frac{5}{2}}$		
$2^1_0K^1_1$ (F''_1)–$2^1_1K^1_2$ (F''_1)	448.0	445.3
$K = 2$, $\Delta_{\frac{3}{2}}$		
$2^0_1K^1_1$ (F''_1)–$2^1_1K^1_2$ (F''_2)	579.4	576.6

† Energies above $J = 0$ of $v_2 = 0$, $^2\Pi_{\frac{3}{2}}$ (F''_1).

(*d*) *Bending vibrations and Renner–Teller coupling*

Figure 7 shows diagrammatically the low-lying spin-vibronic levels in ground and excited state involving the bending vibration for $v_2 \leqslant 2$, and the transitions that have been identified.

In the *excited state* only $v_2 = 1$ has been observed. The frequency of ν'_2 is again obtained from combination differences, listed in table 9.

In the *ground state* the pattern of energy levels involving the bending vibration is complicated, through vibronic interactions between nuclear and electronic motions first described by Teller and Renner. The theory is outlined by Herzberg (1966). Departure from a linear nuclear configuration breaks the orbital degeneracy of the Π state so that Λ ceases to be a good quantum number; however, if spin is neglected $K = (\Lambda + l)$ and is conserved, being the internal component of the total vibronic angular momentum composed of electronic (Λ) and vibrational (l) contributions which are integral only in the linear configuration. Conversely, the nuclei move in the field of an adiabatic double-potential V^+ (upper) and V^- (lower) whose leading (harmonic) terms for small displacements in a Π electronic state are of the form

$$2V^{\pm} = (k_{22} \pm \tfrac{1}{2}\alpha_{22})\,S_2{}^2 + \ldots, \qquad (7)$$

where k_{22} is the harmonic bending force constant in the absence of vibronic coupling and S_2 is a symmetrized displacement coordinate. The strength of the vibronic coupling is measured by Renner's parameter ϵ, where

$$|\epsilon| = \tfrac{1}{2}\alpha_{22}/k_{22} \tag{8}$$

and the sign of ϵ is determined by whether the two non-degenerate electronic states A' and A'' into which the Π state goes on bending correlate with the V^+ and V^- potentials (ϵ positive) or vice versa. In the absence of vibronic coupling ($\alpha = 0$) the vibrational levels of the bending mode would be given in the usual way by

$$G(0, v_2^l, 0) = \omega_2(v_2+1) + gl^2 + \text{anharmonic terms} \tag{9}$$

and it is the purpose of an analysis of observed vibronic structure to extract ω_2 (and g, etc.) if one wishes to continue to think of 'the' bending-frequency of the molecule. It is also the quantity which carries the mass dependence, needed for comparisons between isotopic species.

If now spin-orbit coupling is appreciable the doublet spin-splitting of levels of same K will depend on the Λ content, and as the expectation-value of Λ is in general non-integral the splitting will no longer be simply the $\pm\frac{1}{2}A$ to be found in a diatomic $^2\Pi$ state, but modified in ways expressible in terms of effective spin-vibronic coupling constants A_{eff} and A^* which depend on A, ϵ, ω, v_2 and K. K in turn ceases to be a good quantum number but P ($= K \pm \frac{1}{2}$ for doublet states) is conserved.

Expressions for these coupling constants and the spin-vibronic energy levels have been obtained through perturbation theory by Pople and Hougen, and are given in unified terminology by Herzberg (1966). In particular: for $|\epsilon| < 1$ and levels $K = (v_2+1)$, $\pm\frac{1}{2}$ ('inner' doublets, see figure 7) (Herzberg 1966, equation I, 98)

$$A_{\text{eff}, K} = A[1 - \tfrac{1}{8}\epsilon^2 K(K+1)] \tag{10}$$

and for levels $K < (v_2+1)$, $\pm\frac{1}{2}$ (Herzberg 1966, equation I, 48)

$$A^*_{v_2, K} = [A^2 + \epsilon^2\omega_2^2\{(v_2+1)^2 - K^2\}]^{\frac{1}{2}}. \tag{11}$$

The general expressions for the term values are not reproduced here, but the formulae for the levels $v_2 = 0-2$ are shown in figure 7, which has been drawn for the present case in which $e \approx -0.2$, $\epsilon\omega_2 \approx A$ and $|A| < \omega_2$.

Experimentally what are observed are rospinvibronic term values which are fitted to near-case (a) expansions in $J(J+1)$ of Hill–Van Vleck formulae. The starting points are therefore band origins ν_0 corresponding to the hypothetical levels $J = 0$. These are shown on the right in figure 7, over (a). To obtain the proper rotationless spinvibronic terms ($N = 0$) from ν_0, the J-independent terms in the Hill–Van Vleck formulae have to be added. These formulae have moreover to be slightly modified, replacing $Y(Y-4)$ by $Y(Y-4K/\Lambda)$ (Herzberg 1966, p. 81). The corrections are of order BK^2 and are the first shown on going left in figure 7. The mid-point of the $v_2 = 0$ doublet thus corrected is then taken conventionally as the origin of the orbital vibronic energy scale with respect to which the zero point electronic energies T_{00} of higher electronic states are expressed. The lower component ($^2\Pi_{\frac{3}{2}}$) is, however, taken for convenience as the origin of energy for all the spinvibronic levels of the ground state, shown above (b) in figure 7, for in this way it is much easier to treat, for example, perturbations between near-lying spinvibronic states belonging formally to different $^2\Pi$ sub-states. Finally, the various Renner spin-orbit corrections relate the spinvibronic levels above (b) to the vibrational terms at the left in figure 7 above (c).

PHILOSOPHICAL TRANSACTIONS OF THE ROYAL SOCIETY A MATHEMATICAL, PHYSICAL & ENGINEERING SCIENCES

The combination differences that isolate levels of ν_2'' are also given in table 9. They show that the two Δ components and the lowest Σ component are the three members of the $v_2 = 1$ manifold observed. Of the two $K = 0$ Σ-components expected one behaves largely like an electronic Σ^+ state, the other like Σ^-: not quite, for the + and − labels are again not strictly 'good' labels, so that they are referred to as $^2\Sigma_{\frac{1}{2}}^{(+)}$ and $^2\Sigma_{\frac{1}{2}}^{(-)}$ terms; but sufficiently well to give the two transitions $2_1^0 K_0^0$ $^2\Sigma^+ \rightarrow {}^2\Sigma^{(+)}$ and $^2\Sigma^+ \rightarrow {}^2\Sigma^{(-)}$ widely different intensities. Despite considerable search only the transitions to the lower Σ component has been observed and it must therefore be the $\Sigma^{(+)}$ component. Hence ϵ is negative. A is known to be negative in the $v = 0$ level (see above), and hence the $\Delta_{\frac{3}{2}}$ component is the higher Δ component of the $v_2 = 1$ pair.

TABLE 10. OBSERVED AND CALCULATED ROTATIONLESS SPINVIBRONIC TERM-VALUES FOR LEVELS $v_2 = 0$–2 IN THE GROUND STATE

	$N_2{}^{16}O^+$		$N_2{}^{18}O^+$	
	obs.	calc.	obs.	calc.
constants				
$\omega_2(\mathrm{cm}^{-1})$	—	456.80	—	453.97
$A(\mathrm{cm}^{-1})$	—	−133.59	—	−133.59
ϵ	—	−0.1925	—	−0.1925
intervals/cm^{-1}				
$v_2 = 0$, $(^2\Pi_{\frac{1}{2}}$–$^2\Pi_{\frac{3}{2}})$ $= A_{\mathrm{eff},1}$	132.36	132.36	132.34	132.36
$v_2 = 1$, $(^2\Delta_{\frac{3}{2}}$–$^2\Delta_{\frac{5}{2}})$ $= A_{\mathrm{eff},2}$	130.6	129.88	130.5	129.88
levels $(v_2, K, P = K \pm \frac{1}{2})/\mathrm{cm}^{-1}$				
$(0, 1, 1\frac{1}{2})$	0	0	0	0
$(0, 1, \frac{1}{2})$	132.36	132.36	132.34	132.36
$(1, 0, \frac{1}{2})$ $\Sigma^{(+)}$	412.3	412.55	410.4	410.16
$(1, 2, 2\frac{1}{2})$ $\Delta_{\frac{5}{2}}$	449.2	449.58	446.5	446.80
$(1, 2, 1\frac{1}{2})$ $\Delta_{\frac{3}{2}}$	579.8	579.46	577.0	576.68
$(1, 0, \frac{1}{2})$ $\Sigma^{(-)}$	—	633.41	—	630.14
$(2, 1, 1\frac{1}{2})$ $^2\Pi_{\frac{3}{2}}$		833.50		828.54
$(2, 1, \frac{1}{2})$ $^2\Pi_{\frac{1}{2}}$		839.50		834.54
$(2, 3, 3\frac{1}{2})$ $\Phi_{\frac{7}{2}}$		895.54		889.72
$(2, 3, 2\frac{1}{2})$ $\Phi_{\frac{5}{2}}$		1021.70		1015.88
$(2, 1, \frac{1}{2})$ $^2\Pi_{\frac{1}{2}}$		1115.82		1109.50
$(2, 1, 1\frac{1}{2})$ $^2\Pi_{\frac{3}{2}}$		1121.82		1115.50

The basic data available for the Renner analysis are therefore four spinvibronic intervals for each of $N_2{}^{16}O^+$ and $N_2{}^{18}O^+$. The observed $^2\Pi_{\frac{1}{2}}$–$^2\Pi_{\frac{3}{2}}$ intervals for $\nu_2 = 0$ and the $^2\Delta_{\frac{3}{2}}$–$^2\Delta_{\frac{5}{2}}$ intervals for $\nu_2 = 1$ are so nearly the same for both isotopes that the spin-orbit coupling constant A can be taken as common within experimental error, although not equal to either interval (see equation (10)). Neglecting anharmonicities this leaves essentially four independent intervals to fix in principle four further unknowns: ϵ and ω_2 for $N_2{}^{16}O^+$ and ϵ^i and ω_2^i for $N_2{}^{18}O^+$. To extract ω_2 it is best to place most weight on the interval between the mid-points of the $\nu_2 = 0$, $^2\Pi$ and $\nu_2 = 1$, $^2\Delta$ doublets (see figure 7); and the interval most sensitive to ϵ is then that between $\Sigma^{(+)}$ and $\Delta_{\frac{5}{2}}$ components of $\nu_2 = 1$. Analysed in this way, by iteration, the best fit of the eight intervals to five parameters is obtained with $\epsilon = -0.19336$ and $\epsilon^i = -0.19157$. The difference between these is, however, no greater than the uncertainties introduced by the neglect in equation (9) of the terms in $g\langle l\rangle^2$ and anharmonicities, and probably in the theory of the Renner coupling of terms in higher orders of perturbation theory. ϵ was therefore

constrained to a common value for both isotopes of -0.1925, as also required for adiabatic potentials theoretically, and observed and calculated spinvibronic term values are given in table 10. To extend the analysis by searching for the higher levels not yet identified, the vibronic energies of table 10 may be readily converted to rovibronic origins by adding the appropriate K-dependent corrections shown in figure 7.

One such additional assignment involves a moderately prominent pair of sub-bands having heads at 28558.8 and 28432.2 cm^{-1}. These are almost certainly the sub-bands $2_2^2 K_3^2$ $^2\Delta$–$^2\Phi_{\frac{7}{2}}$ and $^2\Delta$–$^2\Phi_{\frac{5}{2}}$ respectively, lying 330.9 and 337.7 cm^{-1} to the violet of the corresponding 0–0 sub-bands. On the assumption that both lower and upper states are harmonic in ν_2, the expected positions of the sub-bands are 0–0 + 336.8 and 341.4 cm^{-1} respectively. The observed separation of 126.6 cm^{-1} compares with 128.6 cm^{-1} expected. However, as none of the levels has been identified a second time in the spectrum the assignments cannot be further checked.

The frequencies of the bending fundamentals are also included in table 11 as well as the harmonic isotopic ratio $\rho(\nu_2)$,

$$\rho(\nu_2) = \nu_2^i/\nu_2 = (m_O M^i B_e/m_O^i M B_e^i)^{\frac{1}{2}}$$

calculated using values of B_0 instead of the poorly determined or unavailable B_e.

TABLE 11. FUNDAMENTAL VIBRATIONAL FREQUENCIES/cm^{-1}

		N_2O^+			N_2O
		excited state	ground state		ground state
		$\tilde{A}\,^2\Sigma^+$	$^2\Pi_{\frac{1}{2}}$ $\tilde{X}$	$^2\Pi_{\frac{3}{2}}$	$\tilde{X}\,^1\Sigma^+$
$N_2{}^{16}O$	ν_1	1345.52	1126.42	1126.51	1284.91†
	ν_2	614.1	456.8		588.77†
	ν_3	2451.7	1737.7	1737.6	2223.76†
$N_2{}^{18}O$	ν_1	1304.59	1088.3	‡	1255§
	ν_2	610.2	454.0		?
	ν_3	2440.3	1734.7	1736.5	2219.68‖
$\rho(\nu_1\,\nu_3)$¶	obs.	0.9651	0.9645		0.9749
	calc.	0.9639	0.9639		0.9639
$\rho(\nu_2)$	obs.	0.9936	0.9938		—
	calc.	0.9917	0.9919		—
x_{11}^0		—	−14.2		−4.23†

zero-point isotope shift, $\Delta T_{00}(N_2{}^{16}O^+–N_2{}^{18}O^+)$:
obs. 7.38
calc.†† 7.17

† Pliva (1968).
‡ Heavily perturbed, not analysed.
‖ Plyler, Tidwell & Maki (1964).
§ From crystal Raman spectrum: Anderson & Sun (1971).
¶ Product rule ratios.
†† Harmonic approximation, using fundamental frequencies uncorrected for anharmonicities, means of values for both $^2\Pi$ components where available.

(e) *Perturbations*

The dependence in the *ground state* of rotational constants and vibrational energies on ν_1 seen in figures 4 and 6 show that the levels of ν_1 are strongly perturbed in the lower, $^2\Pi_{\frac{3}{2}}$ spin components, and much less so or even negligibly in the upper, $^2\Pi_{\frac{1}{2}}$ spin components. The levels

PHILOSOPHICAL TRANSACTIONS OF THE ROYAL SOCIETY A MATHEMATICAL, PHYSICAL & ENGINEERING SCIENCES

responsible must be Π components of the $2\nu_2$ Renner manifold. The expected positions of all the Π spinvibronic origins ($J = 0$) calculated from the constants of table 10, neglecting anharmonicities, and the observed levels of ν_1'' are given in order of frequencies in table 12.

This table shows that the level $\nu_1\,{}^2\Pi_{\frac{3}{2}}$ of $N_2{}^{16}O^+$ is close to and just above the two upper Π levels of $2\nu_2$, and particularly the $\Pi_{\frac{3}{2}}$ level with which it might therefore be expected to be in close Fermi resonance. Theory shows however that Fermi resonance is expected to be strong only between states of some (signed) quantum numbers Λ, l and Σ individually (Hougen 1962; Johns 1961) which in the present case are $\nu_1(F_1)$ and the *lower* level $2\nu_2$, $\Pi_{\frac{3}{2}}$, 300 cm^{-1} below; and as thus expected, the effects of Fermi-like homogeneous interactions are indeed small, leading to little displacement of the origin from its unperturbed position as shown in figure 6.

TABLE 12. SPINVIBRONIC ORIGINS OF THE Π-COMPONENTS OF ν_1'' AND $2\nu_2''/cm^{-1}$

$N_2{}^{16}O^+$		$N_2{}^{18}O^+$	
$2\nu_2$, $\Pi_{\frac{3}{2}}$ (lower)	833.50	$2\nu_2$, $\Pi_{\frac{3}{2}}$ (lower)	828.54
$\Pi_{\frac{1}{2}}$ (lower)	840.32	$\Pi_{\frac{1}{2}}$ (lower)	835.22
$\Pi_{\frac{1}{2}}$ (upper)	1116.64	ν_1, $\Pi_{\frac{3}{2}}$ (F_1)	1083.3
$\Pi_{\frac{3}{2}}$ (upper)	1121.82	$2\nu_2$, $\Pi_{\frac{1}{2}}$ (upper)	1110.18
ν_1, $\Pi_{\frac{3}{2}}$ (F_1)	1126.51	$\Pi_{\frac{3}{2}}$ (upper)	1115.50
$\Pi_{\frac{1}{2}}$ (F_2)	1259.60	ν_1, $\Pi_{\frac{1}{2}}$ (F_2)	1221.44

Levels of $2\nu_2$ calculated from the constants of table 10 neglecting anharmonicities.

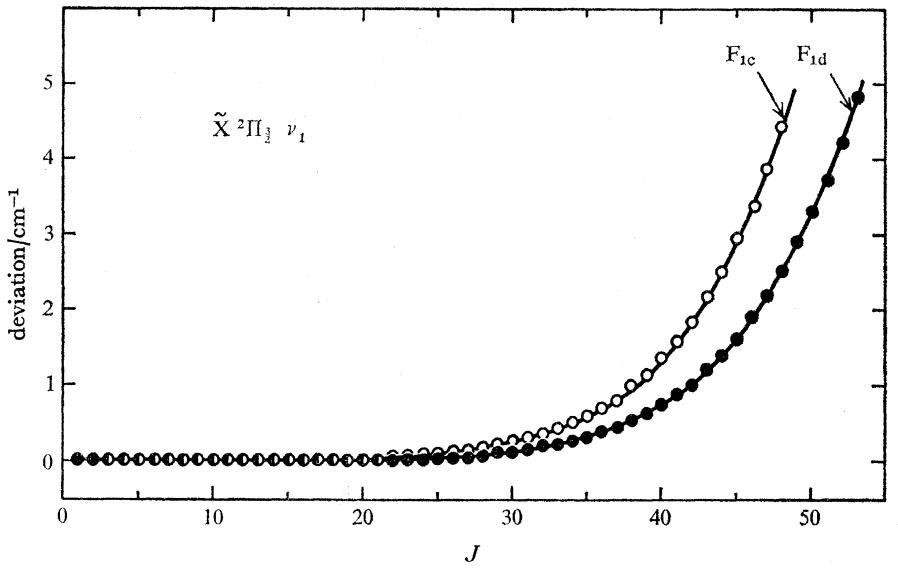

FIGURE 8. Deviations of rotational levels from their expected positions in the two Kramers sub-states of $\tilde{X}\,{}^2\Pi_{\frac{3}{2}}$, ν_1, due to a perturbation by one of the members of the $2\nu_2$ manifold.

The perturbations are therefore rotational. Their course is shown in more detail in figure 8. Up to about $J = 20\frac{1}{2}$ the levels can be represented by an effective B value in the normal way, given in table 2. Thereafter they are displaced upwards from their expected positions, and the residual degeneracy of c and d components split as an apparent Λ doubling. This indicates that the perturbing level is probably principally the upper $\Pi_{\frac{1}{2}}$ level.

In $N_2{}^{18}O^+$ the level ν_1 (F_1) is now expected to lie below the two upper Π levels of $2\nu_2$ (table 12). In fact it appears to be very close to the $\Pi_{\frac{1}{2}}$ level, for the perturbations are now so strong and

irregular that the simple branch-structure of the band 1_1^0 is lost, with the appearance of numerous heads in fragmentary branches. The perturbations were not analysed further. The difference in the relative positions of ν_1'' and $2\nu_2''$ in the two isotopes appears to have even greater effects in the next quantum up, which may be seen in figure 6; the origins of $2\nu_1''$ are displaced in opposite senses. Table 12 shows that in both isotopes the upper spin component $\Pi_{\frac{1}{2}}(F_2)$ of ν_1'' is well above all the levels of $2\nu_2''$ and hence its overtones behave effectively as unperturbed. This difference in the regularities of the levels of ν_1'' in the two spin components is strikingly similar to the behaviour observed in CO_2^+ (Mrozowski 1947).

Perturbations of a different kind are observed in the $^2\Pi_{\frac{3}{2}}(F_1)$ component of ν_3 in the ground-state of $N_2{}^{16}O^+$. The displacement of the levels from the positions expected with the B value given in table 2 are shown in figure 9. Again there is a linear splitting of the Λ doublet degeneracy, of the form expected in a $\Pi_{\frac{1}{2}}$ state but with an apparent doubling constant p an order of magnitude too large. This suggests a Coriolis perturbation (Herzberg 1945, p. 379) and the level responsible is most probably $(\nu_1''+\nu_2'')^2\Sigma_{\frac{1}{2}}^{(-)}$.

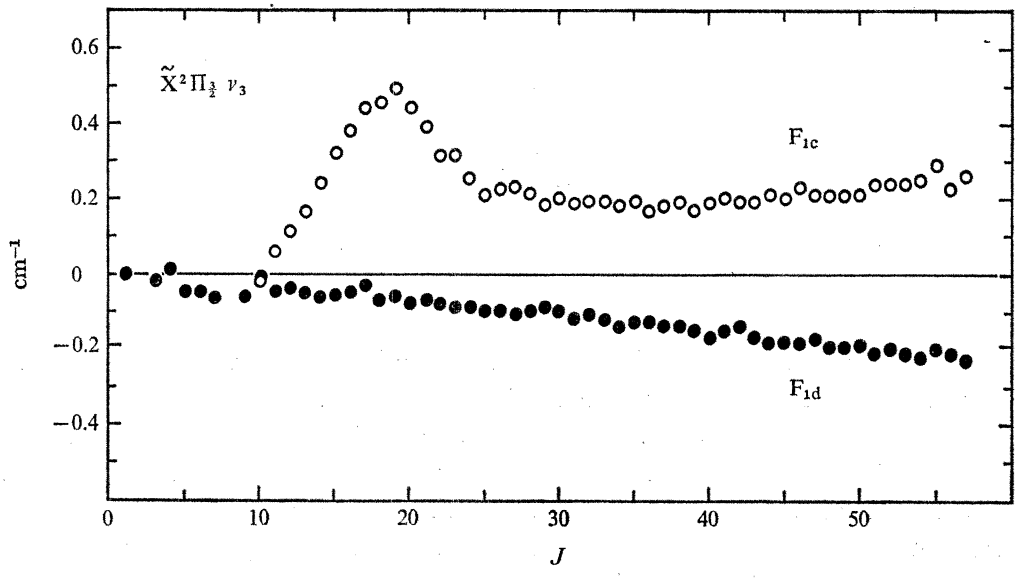

FIGURE 9. Perturbations in $\tilde{X}^2\Pi_{\frac{3}{2}}$, ν_3, giving rise to anomalous Λ doubling and displacement of the levels F_2 around $J = 19$. The ordinate gives the deviations from expected positions calculated with $p = q = 0$, $D_v = D_0$.

4. MOLECULAR STRUCTURE

We discuss here the available information on the potential surfaces of N_2O^+ in its two states: the locations of the minima – bond distances; curvatures near the minima – force fields; and dissociation limits.

(*a*) *Bond distances*

The only precisely determined moments of inertia are those in the zero point levels, and these may be combined from the two isotopes to solve for the mean zero point bond distances r_0. As is well known, the difficulty in determining the bond distances separately in molecules like N_2O lies in the fact that the middle atom is quite close to the molecular centre of gravity and

contributes little to the moments of inertia. To assess the uncertainties in the bond distances individually it is most convenient to solve rather for their sums and differences,

$$R_1 = [r_0(\text{N—O}) - r_0(\text{N—N})],$$

$$R_2 = [r_0(\text{N—O}) + r_0(\text{N—N})],$$

and this can be done graphically by the method used for N_2O by Griggs *et al.* (1968), who give the equations.

TABLE 13. MOMENTS OF INERTIA I_0/a.m.u. Å^2 AND BOND DISTANCES r_0/Å

		$N_2{}^{16}O^+$		$N_2{}^{18}O^+$
I_0	$\tilde{A}\,^2\Sigma^+$	38.9319 (36)		41.2073 (40)
	$\tilde{X}\,^2\Pi$	40.9580 (50)		43.3700 (56)
		R_1		R_2
		$[= r(\text{N—O}) - r(\text{N—N})]$		$[= r(\text{N—O}) + r(\text{N—N})]$
R	$\tilde{A}\,^2\Sigma^+$	0.001 (12)		2.28186 (36)
	$\tilde{X}\,^2\Pi$	0.030 (18)		2.33981 (61)
		r(N—N)		r(N—O)
N_2O^+, $\tilde{A}\,^2\Sigma^+$, r_0		$1.140_2 \pm 0.006$		$1.141_6 \pm 0.006$
$\tilde{X}\,^2\Pi$, r_0		$1.154_8 \pm 0.009$		$1.185_0 \pm 0.009$
N_2O, $\tilde{X}\,^1\Sigma^+$, r_0		1.1289	†	1.1912
r_e		1.1266	‡	1.1856

† Mean for 5 isotopes, values ranging over ± 0.0022; Costain (1958).
‡ Griggs *et al.* (1968).

The moments of inertia are obtained from the rotational constants with the conversion factor used by Herzberg (1966), and are listed in table 13. Atomic masses were taken from Wapstra (1955), corrected to $^{12}C = 12$. For each moment of inertia a plot of R_2 against R_1 gives a curve; for two isotopic moments the intersection of the curves specifies the structure. The curves for the ground and excited states of N_2O^+ are shown in figure 10 and the bond distances obtained from them are listed in table 13. It can be easily seen that the sum of the bond distances is determined about 30 times more precisely than either of them individually.

For comparison, values of r_0 and r_e are included in table 13 for the ground state of neutral N_2O. The uncertainties in the meaning of r_0 structures are discussed fully by Costain (1958) and apply equally well to N_2O^+. They are, however, probably less, in the region of ± 0.003 Å, than the uncertainties arising here from the limited precision of the rotational constants B_0.

(*b*) *Force constants*

There is not enough information to make the first order anharmonic corrections to the fundamental vibrational frequencies $\nu_{1,2,3}$ needed to derive the zeroth order harmonic frequencies ω, and so the best that can be done is to use the ν as if they were harmonic frequencies in calculating an effective harmonic force field. In a simple harmonic valence force field with only principal force constants f_{11} and f_{22} for the N—N and N—O bonds respectively, the two frequencies ν_1 and ν_3 available for each isotope do not give real solutions for f_{11} and f_{22} in the ground state of the ion. This is as in the case of N_2O itself (Penney & Sutherland 1936) and in

NCO (Dixon 1960), and indicates that there is appreciable coupling between the bonds. In the excited state of N_2O^+ real solutions can be found:

$$f_{11}(\text{N—N}) = 18.91 \quad \text{and} \quad f_{22}(\text{N—O}) = 14.24 \times 10^5 \text{ dyn cm}^{-1}.$$

Combining the data from both isotopes (only three of the four stretching frequencies being independent because of the product rule) one can solve for the three harmonic stretching force constants of the complete valence force field. The bending vibration shows an isotopic frequency shift so close to that expected from its product rule (table 11) that it provides essentially only one item of information to fix the bending force field; and hence, neglecting bend–stretch interactions, the potential becomes

$$2V = f_{11}\Delta r(\text{N—N})^2 + f_{22}\Delta r(\text{N—O})^2 + f_{12}\Delta r(\text{N—N})\,\Delta r(\text{N—O}) + f_{\theta\theta}\Delta\theta^2, \qquad (12)$$

where θ measures the departure from linearity. The equations relating the vibrational frequencies to the force field are given by Richardson & Wilson (1950) for the stretching motions,

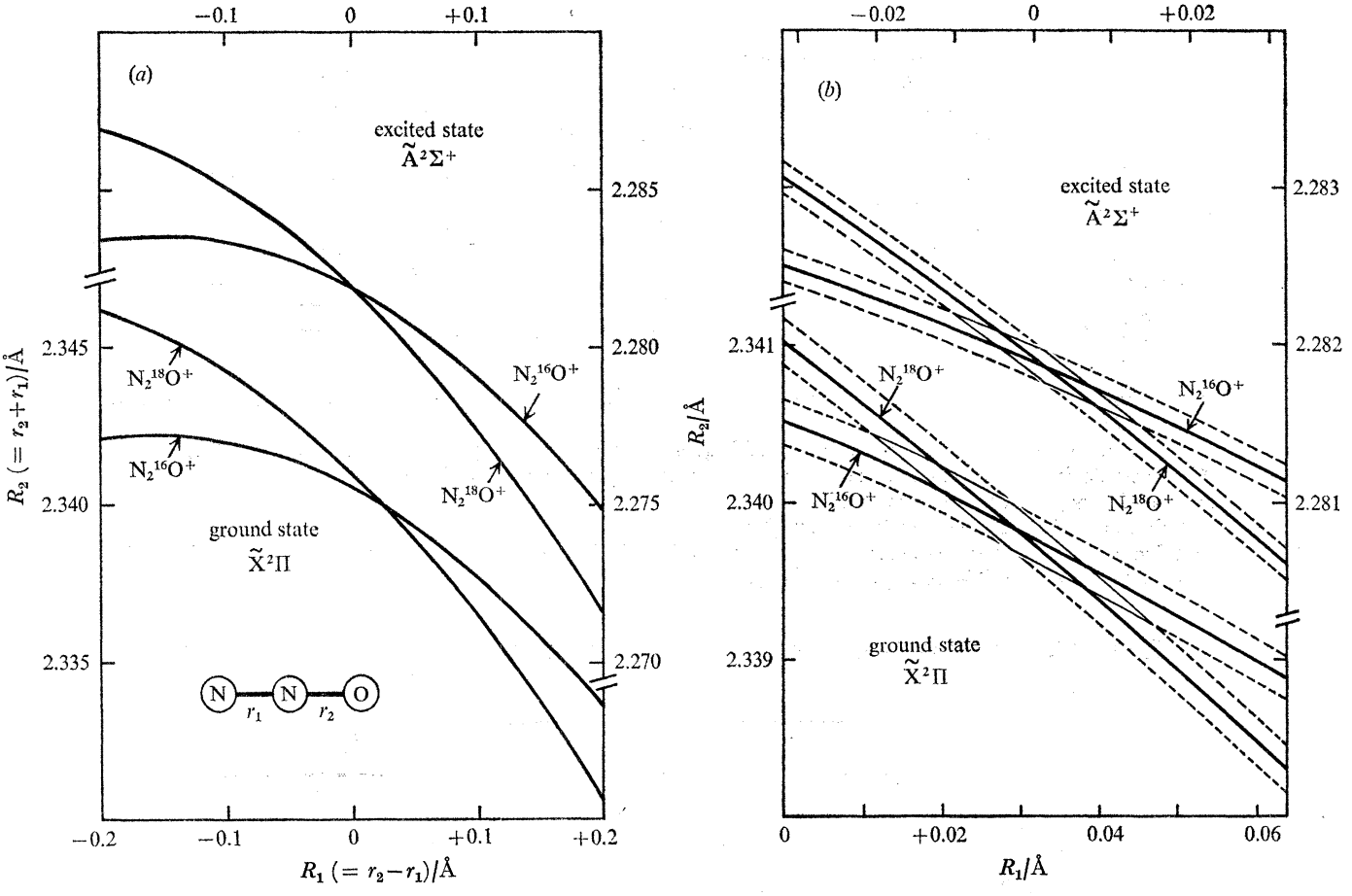

FIGURE 10. Graphical display of the determination of bond distances r_0 from rotational constants B_0. Each curve represents the values of $R_1 = (r_2 - r_1)$ and $R_2 = (r_2 + r_1)$ consistent with one isotopic B_0. Note the difference in scales for R_1 and R_2. (*a*) Small scales. (*b*) The same curves in the regions of cross-over enlarged. Dotted lines represent the uncertainties in the experimental value of B_0, and their intersections the consequent uncertainties in R_1 and R_2.

and Grenier–Besson (1956) for the bending motions. The latter involve additionally the equilibrium bond lengths and moments of inertia but the use here of the zero point values r_0 and I_0 introduces no appreciable error.

Substituting isotopically at the oxygen atom determines f_{22} unambiguously, but the equations are such that two solutions are possible for f_{11} and f_{12}. The force constants obtained are shown in table 14. For comparison, a similar set is included for neutral N_2O. It was derived to give the best overall fit to the fundamental frequencies of a number of isotopes by Griggs, Rao, Jones & Potter (1965). Finally, the harmonic force field calculated from zero order frequencies ω corrected for anharmonicities is given in the last column. The choice between solutions (1) and (2) is in almost all cases clear on grounds of reasonable magnitudes: solutions (2) tend to include unacceptably large interaction constants. The choice is, however, independently supported by additional information which lies in the centrifugal distortion constants D. These may be calculated from each force field through the equation given by Verdier & Wilson (1959); and calculated values are compared with experimental values in table 15.

The meaningfulness of the force constants in table 14 is not easy to assess. Quite small changes

TABLE 14. QUADRATIC FORCE CONSTANTS/dyn cm^{-1}‖

	N_2O^+				N_2O		
	$\tilde{A}\,^2\Sigma^+$		$\tilde{X}\,^2\Pi$		$\tilde{X}\,^1\Sigma^+$		
	(1)†	(2)†	(1)†	(2)†	(1)‡	(2)‡	(3)§
$10^{-5}f_{11}$	19.33	(32.99)	12.43	(15.90)	18.01	(26.52)	18.31
$10^{-5}f_{22}$	13.93		8.04		11.33		11.94
$10^{-5}f_{12}$	0.13	(13.79)	2.29	(5.75)	1.41	(9.92)	1.07
$10^{11}f_{\theta\theta}$/erg rad^{-1}‖	0.691		0.401			0.654	0.666
$10^{-5}f_{\theta\theta}/r_1r_2$	0.530		0.293		0.486		0.499
$10^{-5}f^{+}_{\theta\theta}/r_1r_2$¶	—		0.350			—	
$10^{-5}f^{-}_{\theta\theta}/r_1r_2$¶	—		0.237			—	
$10^{-5}\alpha_{\theta\theta}/r_1r_2$¶	—		0.113			—	

† Solutions (1) and (2) of the equations for f_{ij} in terms of fundamental frequencies given in table 11: see text. Solutions (1) adopted.

‡ Solutions (1) and (2) giving best mean fit of frequencies of several isotopes as derived by Griggs *et al.* (1965).

§ Harmonic force constants from zero order harmonic frequencies and equilibrium bond lengths as given by Griggs *et al.* (1965, 1968) and Pliva (1968).

‖ 1 dyn = 10^{-5} N; 10^{-11} erg rad^{-1} = 10^{-18} J rad^{-1}.

¶ Effective quadratic force-constants for separate adiabatic Renner-decoupled potentials $V^{(+)}$ and $V^{(-)}$, split by $\alpha_{\theta\theta} = 2\epsilon f_{\theta\theta}$. $r_1 = r_0$(N—N), $r_2 = r_0$(N—O).

TABLE 15. CALCULATED AND OBSERVED CENTRIFUGAL DISTORTION CONSTANTS D_v/cm^{-1}

		N_2O^+				N_2O		
		$\tilde{A}\,^2\Sigma^+$		$\tilde{X}\,^2\Pi$		$\tilde{X}\,^1\Sigma^+$		
		(1)†	(2)	(1)	(2)	(1)	(2)	(3)
$N_2{}^{16}O^+$	10^7D_0(calc.)	1.77	1.07	2.09	1.67	1.73	1.22	1.725‡
	10^7D_0(obs.)	1.75		1.90		1.79		1.719§
$N_2{}^{18}O^+$	10^7D_0(calc.)	1.68	1.15	1.80	1.45			
	10^7D_0(obs.)	1.60		1.76				

† Numbers (1), (2) and (3) refer to the force fields of table 14.

‡ D_e.

§ D_e, from Pliva (1968).

in the frequencies used to calculate them produce large but correlated changes among them up to ±10%, to which the calculated centrifugal constants are quite insensitive. The number of digits quoted is that necessary to reproduce the input frequencies. Hopefully, the neglect of anharmonic corrections affects mainly the absolute, much less the relative, magnitudes; and a comparison of columns (1) and (3) under neutral N_2O gives some support to this.

TABLE 16. DISSOCIATION LIMITS AND PRODUCTS OF N_2O AND N_2O^+.

		energies†		
no.	products	eV	cm^{-1}	kcal mol^{-1}
19	$N_2^+(B\,^2\Sigma_u^+)+O(^3P_2)$	20.421 (10)	60 710 (80)	173.58 (23)
18	$N_2^+(A\,^2\Pi_u)+O(^1D)$	20.331 (10)	59 990 (20)	
17	$N_2(X\,^1\Sigma_g^+)+O^+(^2P)$	20.306 (10)	59 780 (80)	
16	$NO(X\,^2\Pi)+N^+(^3P_0)$	19.472 (20)	53 055 (160)	151.70 (47)
15	$N_2^+(X\,^2\Sigma_g^+)+O(^1D)$	19.218 (10)	51 010 (80)	
14	$N_2(X\,^1\Sigma_g^+)+O^+(^2D)$	18.614 (10)	46 130 (80)	
13	$N_2^+(A\,^2\Pi_u)+O(^3P_2)$	18.364 (10)	44 120 (80)	126.15 (23)
12	$NO^+(^1\Sigma^+)+N(^2P)$	17.763 (20)	39 270 (160)	
11	$N_2^+(X\,^2\Sigma_g^+)+O(^3P_2)$	17.251 (10)	35 140 (80)	100.48 (23)
10	$NO^+(X\,^1\Sigma^+)+N(^2D)$	16.571 (20)	29 660 (160)	
9	$N_2(X\,^1\Sigma_g^+)+O^+(^4S)$	15.289 (10)	19 310 (80)	55.22 (23)
8	$NO^+(X\,^1\Sigma^+)+N(^4S)$	14.187 (20)	10 430 (160)	29.83 (47)
7	$N_2O^+(\tilde{X}\,^2\Pi)$ —	12.893 (5)	0 (= 103 990) (40)	0 (= 292.32) (12)
6	$N(^4S)+N(^4S)+O(^3P_2)$	11.432 (10)	92 204 (82)	263.62 (24)
5	$NO(X\,^2\Pi_{\frac{1}{2}})+N(^4S)$	4.924 (15)	39 720 (120)	113.56 (34)
4	$N_2(X\,^1\Sigma_g^+)+O(^1D)$	3.639 (50)	29 350 (40)	83.92 (12)
3	$N_2(X\,^1\Sigma_g^+)+O(^3P_2)$	1.672 (5)	13 485 (42)	38.55 (12)
2	$N_2O(\tilde{X}\,^1\Sigma^+)$ —	0	0	0
1	$N_2(g)^0+\frac{1}{2}O_2(g)^0$	−0.8859 (43)	−7 145 (35)	−20.43 (10)

† Conversion-factors as given by Herzberg (1966). 1 cal = 4.1840 J.

‡ Basic reaction-energies used in computation:

I.P.(N_2O): see table 1. Two Rydberg series going to $\tilde{X}$ and $\tilde{A}$ of N_2O^+, quoted in Herzberg (1966).

I.P.(N_2): Worley–Jenkins Rydberg series to a limit at 125665.8 (±1?) cm^{-1}; accuracy probably governed by uncertainties in far-u.v. calibration.

I.P.(NO): Rydberg limit at 74720 ± 5 cm^{-1} (Jungen & Miescher 1969).

$D_0^0(O_2)$: 41260 ± 15 cm^{-1} (Brix & Herzberg 1954; see Rosen 1970).

$D_0^0(N_2)$: 78719 ± 40 cm^{-1} (Lofthus, in Rosen 1970).

$D_0^0(NO)$: 52484 ± 41 cm^{-1}, from $\Delta H_f^0(NO)$ (Frisch 1962, quoted in Stull & Prophet 1971), $D_0^0(N_2)$ and $D_0^0(O_2)$.

$\Delta H_f^0(N_2O)$: −20.43 ± 0.10 kcal mol^{-1} (Stull & Prophet 1971).

The last three rows of table 14 give the effective quadratic force constants and their difference for the two separate adiabatic potentials of the ground state of the ion whose coupling leads to the dynamic Renner–Teller effect analysed above (Herzberg 1966, p. 27, equation I, 32 and p. 30).

(*c*) *Dissociation limits, predissociation and products*

The molecule nitrous oxide and its ions is one of the few polyatomic systems in which all possible dissociation limits are known with any precision. The energies (in the zero point levels where appropriate) are listed in table 16 for the lower limits in both neutral and ionized species, and the states of the molecular ion and its dissociation products are shown diagrammatically in figure 11. The basic elementary reaction energies needed to calculate these energies are also given in table 16; atomic and diatomic excitation energies are taken from standard tables (Moore 1949; Rosen 1970). In $^2\Pi$ and ^3P states the energies are those of the lowest component; in other multiplets, mainly atomic, the splittings are negligible. The dissociation energies and their correlations with molecular ionic states were previously discussed by Lorquet & Cadet (1971).

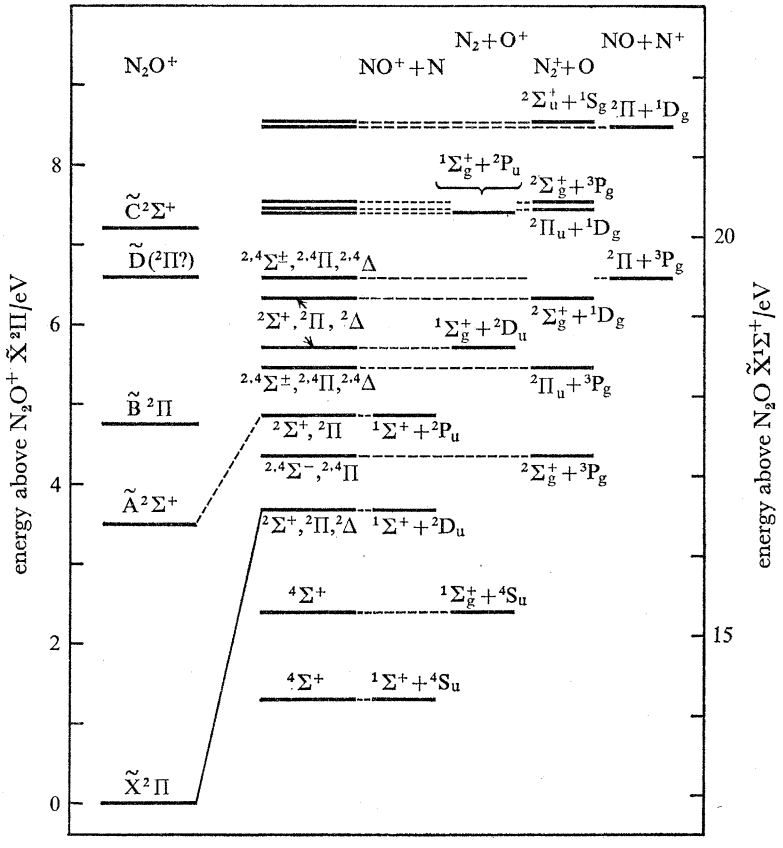

FIGURE 11. States of N_2O^+ and possible dissociation products.

Dissociation of the ground state of N_2O^+ into the lowest two limits is spin forbidden (figure 11), just as the ground state of neutral N_2O must go spin adiabatically to the second limit (no. 4 in table 16).

The excited state of N_2O^+ could in principle correlate with one of the states of the next limit up, but as this lies only $1430 \pm 170\ \mathrm{cm}^{-1}$ higher, it is ruled out by the rigidity of the

molecule. Thus, in the neighbourhood of its equilibrium configuration in the $\tilde{A}\,^2\Sigma$ state the molecule behaves as if it would like to dissociate into a high-lying dissociation channel. There is no shortage of possibilities and little help with the choice. Even so, there remains a non-crossing conflict with the $^2\Sigma^+$ state from the third ionic limit, and there may be some evidence for this from the emission spectrum. The highest vibrational level in the $\tilde{A}$ state from which fluorescence has been observed is $2\nu_1$, 2681 cm^{-1} above zero point, and this is so weak that it seems unlikely to reflect only the rather low Condon factor in the primary excitation (Rosenstock 1971; Hollas & Sutherley 1973; Turner *et al.* 1970, figure 4. 3). It seems rather that the fluorescence may in part be quenched by competition from a non-radiative process, which can only be predissociation. There may be some additional evidence to this effect to be seen already in the levels ν_1 and ν_3, 1345 and 2452 cm^{-1} above zero point, in the fluorescence lifetime measurements of Fink & Welge (1968) (see also Smith 1969). All six transitions observed from the zero point of $\tilde{A}\,^2\Sigma^+$ gave a lifetime of $2.28–2.34 \times 10^{-7}$ s ($f = 0.0041$) whereas another six, four of them at the time unassigned but now known to originate in ν_1' and ν_3', give values in the range $1.87–1.92 \times 10^{-7}$ s. Additional measurements of single vibronic level fluorescence lifetimes, including $2\nu_1'$, would be valuable. A slow predissociation with a lifetime of about 5×10^{-7} s is reported by Coleman, Delderfield & Reuben (1969), based on the appearance of metastable peaks in the mass spectrum of N_2O. The products are $NO^+ + N$, although there is no way of telling whether it is ground state $N(^4S)$ or metastable excited $N(^2D)$, corresponding to the lowest and third dissociation limits of N_2O^+. It seems probable however that the state being predissociated is the $\tilde{A}\,^2\Sigma$ state. The weak predissociation observed through direct photodissociation of the ion in a cyclotron (Dunbar 1971) must be into the continuum of ground state products, for its threshold lies below 2 eV above the ground state of the ion.

Note added in proof (17 June 1974): The weak predissociation of N_2O^+, $\tilde{A}^2\Sigma^+$ in $v_{1,3} > 0$ has been recently confirmed in photoelectronic and photoionic coincidence measurements by Eland (1973), who deduces a predissociative lifetime of $4.1 \pm 0.9 \times 10^{-7}$ s.

(*d*) *Electronic structure*

There can be no doubt that the four states $\tilde{X}$, $\tilde{A}$, $\tilde{B}$ and $\tilde{C}$ of N_2O^+ are the ones expected as the result of removing an electron from one of the four outermost filled molecular orbitals of nitrous oxide (see table 1). It is here however not as easy to describe individual electrons as bonding or antibonding as it is in, say, isoelectronic CO_2^+, for calculations of conventional type show that the 2π and 7σ orbitals are highly localized on the terminal oxygen and nitrogen atoms respectively (Horsely & Fink 1969). Ionization must therefore lead to considerable changes in dipole moment in the molecule, and this may be regarded as a major contributor to the relative changes in r(NN) and r(NO) shown in table 13, and perhaps the reason for the lack of any simple relation between the bond distances and bond force constants shown in table 14. The only point that emerges clearly is that removal of a 7σ electron, which would probably be usually regarded as a 'lone pair' electron, leads to a general contraction and stiffening of the molecule as a whole in the same way as has hitherto been known most strikingly in diatomic molecules. The calculations reproduce the spin-orbit coupling constant of the ground state of N_2O^+ quite well (Horsely & Hall 1973), again indicating the 2π electrons to be mainly on the oxygen.

Configuration interaction calculations (Lorquet & Cadet 1971; Horsely & Hall 1973) lend

support to the existence of further low lying $^2\Pi$ states arising from configuration $\ldots 2\pi^2.3\pi^*$ claimed to have been detected in the photoelectron spectrum of N_2O (see table 1). The correlation table in figure 11 certainly indicates no lack of low lying $^2\Pi$ state limits, most of which appear in fact to be at energies below those claimed for the molecular $^2\Pi$ states seen in the photoelectron spectrum. The question arises therefore whether the latter are stable in the linear configuration, or even at all. A source of stabilization could be bending of the molecule, as in the case of low lying states of NO_2 in which the analogous $2\pi^*$ orbital also contains one electron. It seems that perhaps the only way to explore these possibilities is by further electronic calculations in the field of a nonlinear nuclear framework.

We thank the University of Melbourne for a Travelling Research Scholarship (F. C.), and the Australian National University for a Visiting Fellowship during which this account was written (J. H. C.).

References

Abernethy, E. R. 1964 M.Sc. Thesis, University of British Columbia.
Anderson, A. & Sun, T. S. 1971 *Chem. Phys. Lett.* **8**, 537.
Anderson, V. M. & Callomon, J. H. 1973 *J. Phys.* (B: *Atom. molec. Phys.*) **6**, 1664.
Brocklehurst, B. 1958 *Nature, Lond.* **182**, 1366.
Callomon, J. H. 1958 *Proc. R. Soc. Lond.* A **244**, 220.
Callomon, J. H. 1959 *Proc. chem. Soc. Lond.* p. 313.
Callomon, J. H. & Creutzberg, F. 1967 *Proc. Int. Conf. Spectroscopy Bombay*, **1**, 171. India: Department Atomic Energy.
Callomon, J. H. & Morgan J. E. 1965 *Proc. phys. Soc. Lond.* **86**, 1091.
Coleman, R. J., Delderfield, J. S. & Reuben, B. G. 1969 *Int. J. Mass Spectrom. Ion Phys.* **2**, 25.
Costain, C. C. 1958 *J. chem. Phys.* **29**, 864.
Creutzberg, F. 1964 Thesis, University of London.
Dayton, I. E., Dalby, F. W. & Bennett, R. G. 1960 *J. chem. Phys.* **33**, 179.
Dibeler, V. H. & Walker, J. A. 1968 *Adv. Mass Spectrometry* **4**, 767.
Dixon, R. N. 1960 *Phil. Trans. R. Soc. Lond.* A **252**, 165.
Dunbar, R. C. 1971 *J. Am. chem. Soc.* **93**, 4354.
Eland, J. H. D. 1973 *Int. J. Mass Spectrom. Ion Phys.* **12**, 389
Fink, E. H. & Welge, K. H. 1968 *Z. Naturf.* A **23**, 358.
Frisch, M. A. 1962 Thesis, University of Wisconsin.
Grenier-Besson, M. L. 1956 *Cahiers Phys.* **69**, 8.
Griggs, J. L., Rao, K. N., Jones, L. H. & Potter, R. M. 1965 *J. molec. Spectrosc.* **18**, 212.
Griggs, J. L., Rao, K. N., Jones, L. H. & Potter, R. M. 1968 *J. molec. Spectrosc.* **25**, 24.
Haugh, M. J. & Bayes, K. D. 1970 *Phys. Rev.* (3) A **2**, 1778.
Herzberg, G. 1945 *Infra-red and Raman spectra of polyatomic molecules*. Princeton: Van Nostrand.
Herzberg, G. 1950 *Spectra of diatomic molecules*, 2nd ed. Princeton: Van Nostrand.
Herzberg, G. 1966 *Electronic spectra of polyatomic molecules*. Princeton: Van Nostrand.
Hollas, J. M. & Sutherley, T. A. 1973 *Chem. phys. Lett.* **21**, 167.
Horani, M. & Leach, S. 1959 *C. r. hebd. Séanc. Acad. Sci., Paris* **248**, 2196.
Horsley, J. A. & Fink, W. H. 1969 *J. Phys.* (B: *Atom. molec. Phys.*) **2**, 1261.
Horsley, J. A. & Hall, J. A. 1973 *Molec. Phys.* **25**, 483.
Hougen, J. T. 1962 *J. chem. Phys.* **37**, 403.
James, T. C. 1964 *J. chem. Phys.* **41**, 631.
Johns, J. W. C. 1961 *Can. J. Phys.* **39**, 1738.
Jungen, C. & Miescher, E. 1969 *Can. J. Phys.* **47**, 1769.
Lorquet, J. C. & Cadet, C. 1971 *Int. J. Mass Spectrom. Ion Phys.* **7**, 245.
Monahan, K. & Wauchop, T. S. 1972 *J. geophys. Res.* **77**, 6262.
Moore, C. E. 1949 *Atomic energy levels*. U.S. Nat. Bur. Stand. Circular 467.
Mrozowski, S. 1941–7 *Phys. Rev.* **72**, 682, 691, and earlier papers.
Mulliken, R. S. 1930 *Rev. mod. Phys.* **2**, 60.
Penney, W. G. & Sutherland, G. B. B. M. 1936 *Proc. R. Soc. Lond.* A **156**, 654.
Pliva, J. 1964 *J. molec. Spectrosc.* **12**, 360.
Pliva, J. 1968 *J. molec. Spectrosc.* **27**, 461.

PHILOSOPHICAL TRANSACTIONS OF THE ROYAL SOCIETY A MATHEMATICAL, PHYSICAL & ENGINEERING SCIENCES

Plyler, E. K., Tidwell, E. D. & Maki, A. G. 1964 *J. Res. natn. Bur. Stand.* A **68**, 79.
Poulizac, M. C. & Druetta, M. 1969 *C. r. hebd. Séanc. Acad. Sci., Paris* B **269**, 114.
Richardson, W. S. & Wilson, E. B. 1950 *J. chem. Phys.* **18**, 694.
Rosen, B. (ed.) 1970 *International tables of selected constants*, 17: *Spectroscopic data relative to diatomic molecules*. Oxford: Pergamon.
Rosenstock, H. M. 1971 *Int. J. Mass Spectrom. Ion Phys.* **7**, 33.
Smith, D. R. & Seddon, W. A. 1969 *Chem. Phys. Lett.* **3**, 640.
Smith, W. H. 1969 *J. chem. Phys.* **51**, 3410.
Stull, D. R. & Prophet, H. 1971 *JANAF thermochemical tables*, 2nd ed. *NSRDS-NBS* **37** (Washington).
Tanaka, Y., Jursa, A. S. & Le Blanc, F. J. 1960 *J. chem. Phys.* **32**, 1205.
Turner, D. W., Baker, C., Baker, A. D. & Brundle, C. R. 1970 *Molecular photoelectron spectroscopy*. London: Wiley-Interscience.
Turner, D. W. & May, D. P. 1967 *J. chem. Phys.* **46**, 1156.
Verdier, P. H. & Wilson, E. B. 1959 *J. chem. Phys.* **30**, 1372.
Wapstra, A. H. & Huizenga, J. R. 1955 *Physica* **21**, 367.
Zawadski, J. 1950 *Discuss. Faraday Soc.* **8**, 140.

PHILOSOPHICAL TRANSACTIONS OF THE ROYAL SOCIETY A MATHEMATICAL, PHYSICAL & ENGINEERING SCIENCES

Appendix. Wavelengths and frequencies of band heads in the spectra of $N_2{}^{16}O^+$ and $N_2{}^{18}O^+$

(*a*) Assigned bands

		$N_2{}^{16}O^+$				$N_2{}^{18}O^+$		
assignment	branch	λ_{air}(head) (*a*)†	ν_{vac}(head) (*b*)	ν_{00} (*c*)	intensity (*d*)	λ_{air}(head) (*a*)	ν_{vac}(head) (*b*)	ν_{00} (*c*)
1_1^2	(Q_1+P_{21})	3356.745	29782.20	29784.2	2	—	—	—
	P_1	58.591	765.84		1	—	—	—
	$(Q_{12}+P_2)$	71.837	648.91	651.2	2	—	—	—
	P_{12}	73.878	630.97		0	—	—	—
1_0^1	(Q_1+P_{21})	3380.454	573.33	575.46	40	3385.974	29525.12	29527.13
	P_1	82.402	556.30		25	87.801	509.19	
	$(Q_{12}+P_2)$	95.787	439.80	442.27	40	401.347	391.68	393.99
	P_{12}	98.048	420.27		20	03.444	373.57	
$1_1^0 3_0^1$	(Q_1+P_{21})	3382.763	553.15	555.1	5	—	—	—
	P_1	84.587	537.22		1	—	—	—
	$(Q_{12}+P_2)$	98.094	419.82	422.0	5	—	—	—
	P_{12}	—	—			—	—	—
$1_0^2 3_1^0$	(Q_1+P_{21})	3427.071	171.07	173.1	3	—	—	—
	P_1	28.909	155.44		2	—	—	—
	$(Q_{12}+P_2)$	42.608	039.42	041.8	2	—	—	—
	P_{12}	—	—			—	—	—
$1_0^1 2_1^0 K_0^0$ $^2\Sigma^+$–$^2\Sigma^{(+)}$	P_2	3428.995	154.71	162.9	10	3434.34	109.3	115.9
	P_1	29.505	150.337		10	34.82	105.3	
3_1^1	(Q_1+P_{21})	3454.200	28941.98	28943.85	25	3456.273	28924.61	‡
	P_1	56.106	926.01		15	58.068	909.60	
	$(Q_{12}+P_2)$	69.988	810.30	812.64	25	72.068	793.04	‡
	P_{12}	72.175	792.15		10	74.111	776.10	
$2_1^1 K_0^1$ $^2\Pi$–$^2\Pi$	P_{21}	3466.163	842.08	844.1	2	—	—	—
	P_2	82.268	708.70	710.9	3	—	—	—
$2_2^2 K_3^3$ $^2\Delta$–$^2\Phi_{\frac{7}{2}}$	Q	3500.551	558.76		15	—	—	—
$^2\Delta$–$^2\Phi_{\frac{5}{2}}$	Q	16.137	432.17		25	—	—	—
1_1^1	(Q_1+P_{21})	3514.300	447.03	448.9	10	—	—	—
	P_1	15.977	433.47		10	—	—	—
	$(Q_{12}+P_2)$	30.835	313.82	315.9	5	—	—	—
	P_{12}	32.872	297.49		15	—	—	—
$2_1^1 K_0^1$ $^2\Pi$–$^2\Sigma^{(+)}$	Q_1	3516.261	431.16	431.2	20	3517.439	421.64	28421.5
	P_2	17.156	423.93		30	18.224	415.30	
	P_1	17.647	419.97		30	18.695	411.50	
$2_1^1 K_2^1$ $^2\Pi$–$^2\Delta_{\frac{5}{2}}$	(Q_1+P_{21})	3520.853	394.09	396.1	50	3521.930	385.40	387.2
	P_1	22.806	378.35		30	23.761	370.66	
	P_1	22.881	377.75		20	23.837	370.04	
$2_1^1 K_2^1$ $^2\Pi$–$^2\Delta_{\frac{3}{2}}$	$(Q_{12}+P_2)$	3537.261	262.38	264.7	30	38.326	253.90	256.0
	P_{12}	39.506	244.45		10	—	—	
	P_{12}	39.609	243.63		5	—	—	
0_0^0	(Q_1+P_{21})	3541.583	227.90	229.94	100	3542.489	220.68	222.52
	P_1	43.535	212.34		70	44.331	206.01	
	$(Q_{12}+P_2)$	58.407	094.44	096.76	100	59.307	087.33	089.40
	P_{12}	60.643	076.80		70	61.399	070.84	
$1_0^1 3_1^0$	(Q_1+P_{21})	3591.443	27836.05	27837.9	5	3597.52	27796.9	
	P_1	93.361	821.16		3			
	$(Q_{21}+P_2)$	3608.503	704.42	706.6	5	3614.65	657.3	
	P_{12}	10.714	687.47		3			
$2_1^0 K_0^0$ $^2\Sigma^+$–$^2\Sigma^{(+)}$	P_2	3594.804	809.99	817.3	30	3595.40	805.4	27811.4
	P_1	95.320	806.00		30	95.88	801.7	

PHILOSOPHICAL TRANSACTIONS OF THE ROYAL SOCIETY A MATHEMATICAL, PHYSICAL & ENGINEERING SCIENCES

APPENDIX (*cont.*)

assignment	branch	$N_2^{16}O^+$ λ_{air}(head) (*a*)†	ν_{vac}(head) (*b*)	ν_{00} (*c*)	intensity (*d*)	$N_2^{18}O^+$ λ_{air}(head) (*a*)	ν_{vac}(head) (*b*)	ν_{00} (*c*)
$1_1^0 3_1^1$	(Q_1+P_{21})	3596.219	27 799.05	27 800.8	15	3593.45	27 820.5	
	P_1	98.043	784.96		10	95.14	807.4	
	$(Q_{12}+P_2)$	3613.444	666.54	668.54	15	3610.43	689.6	
	P_{12}	15.491	650.88		5	12.37	674.8	
1_2^1	(Q_1+P_{21})	3656.161	343.30	345.4	15	50.67	384.4	
	P_1	58.348	326.96		5			
	$(Q_{12}+P_2)$	73.153	216.84	218.5	20	69.92	240.8	
	P_{12}	75.010	203.06		10			
1_1^0	(Q_1+P_{21})	3688.751	101.73	103.44	70	(3683–	‡	‡
	P_1	90.634	087.91		50	3686)		
	$(Q_{12}+P_2)$	3706.971	26 986.53	26 970.34	70	3702.744	26 999.31	27 001.10
	P_{12}	09.030	953.56		50	04.666	985.31	
$1_1^1 3_1^0$	(Q_1+P_{21})	3745.238	692.98	694.7	5	—	—	
	P_1	47.108	679.66		3	—	—	
	$(Q_{12}+P_2)$	63.913	560.55	562.4	2	64.6	556	
	P_{12}	66.007	545.78		2	66.5	542	
$1_2^0 3_1^1$	(Q_1+P_{21})	3746.498	684.01	685.6	5	—	—	
	$(Q_{12}+P_2)$	65.188	551.51	553.3	2	—	—	
3_1^0	(Q_1+P_{21})	3773.859	490.55	492.3	3	74.5	486	
	P_1	75.832	476.71		2	76.4	473	
	$(Q_{12}+P_2)$	92.762	358.98	360.9	2	—	—	
	P_{12}	94.684	345.18		1	—	—	
1_3^1	(Q_1+P_{21})	3802.246	292.78	294.2	3	94.1	349	
	P_1	03.815	281.93		3	95.7	338	
	$(Q_{12}+P_2)$	23.527	146.44	147.9	5	3815.3	203	
	P_{12}	25.274	134.50		3	16.9	192	
1_2^0	(Q_1+P_{21})	3845.379	25 997.68	25 999.8	20	33.0	082	
	P_1	46.919	987.46		10	34.7	070	
	$(Q_{12}+P_2)$	64.167	871.46	873.1	20	54.2	25 938	
	P_{12}	67.181	858.63		15	56.0	926	
$1_2^1 3_1^0$	(Q_1+P_{21})	3908.535	577.79	579.3	5	—	—	
	P_1	10.366	565.81		3	—	—	
	$(Q_{12}+P_2)$	28.861	445.47	447.1	4	—	—	
	P_{12}	30.860	432.52		2	—	—	
$1_1^0 3_1^0$	(Q_1+P_{21})	3944.029	347.60	349.2	4	3938.6	383	
	P_1	45.963	335.18		3	40.6	370	
	$(Q_{12}+P_2)$	64.745	215.17	216.9	3	59.2	251	
	P_{12}	66.902	201.46		1	61.1	238	
1_4^1	(Q_1+P_{21})	3959.962	25 245.63	25 246.9	2	—	—	
	P_1	61.485	235.92		1	—	—	
	$(Q_{12}+P_2)$	83.146	098.68	100.0	2	—	—	
	P_{12}	84.820	088.14		0	—	—	
1_3^0	(Q_1+P_{21})	4007.304	24 947.38	24 948.4	5	91.8	044	
	P_1	08.955	937.11		4	93.5	034	
	$(Q_{12}+P_2)$	30.962	800.97	802.4	5	4015.2	24 898	
	P_{12}	32.772	789.84		2	16.8	888	
$1_2^0 3_1^0$	(Q_1+P_{21})	4125.531	232.47	233.9	2	—	—	
	P_1	27.446	221.23		1	—	—	
	$(Q_{12}+P_2)$	48.194	100.08	101.6	2	—	—	
	P_{12}	50.275	088.00		1	—	—	
1_4^0	(Q_1+P_{21})	4182.868	23 900.31	23 901.5	0	—	—	
	$(Q_{12}+P_2)$	4208.762	753.26	754.5	0	—	—	

PHILOSOPHICAL TRANSACTIONS OF THE ROYAL SOCIETY A MATHEMATICAL, PHYSICAL & ENGINEERING SCIENCES

Appendix (*cont.*)

(*b*) Unassigned bands

$N_2{}^{16}O^+$			$N_2{}^{18}O^+$		
λ_{air}(head) (*a*)†	ν_{vac}(head) (*b*)	intensity (*d*)	λ_{air}(head) (*a*)	ν_{vac}(head) (*b*)	intensity (*d*)
3362.053	29 735.19	2	3495.534	28 599.75	10
65.173	716.15	1	96.831	589.14	10
67.691	685.41	1	3501.779	548.74	10
69.975	665.29	1	03.375	535.74	10
71.521	651.69	3	16.269	431.10	15
77.039	603.24	2	16.822	426.63	15
79.047	585.65	1	17.128	424.14	10
80.547	572.52	2	17.668	419.79	10
82.702	553.68	3	94.20	27 814.7	5
85.117	532.60	0	96.06	800.3	2
89.858	491.30	1	99.37	774.7	5
91.695	475.32	1	3602.17	753.1	5
3404.359	365.58	1	12.65	672.6	5
31.625	132.36	3	16.57	642.6	2
32.313	126.52	2	52.08	373.9	5
32.832	122.12	2	52.24	372.7	10
35.493	099.56	5	53.99	359.5	2
37.411	083.33	2	54.38	356.6	2
50.910	28 969.56	5	54.95	352.4	15
53.281	949.68	2	56.16	343.3	10
80.734	721.35	3	56.97	337.3	5
83.134	701.56	2	57.18	335.7	5
94.101	611.48	10	57.91	330.2	10
94.293	609.90	5	58.46	326.1	5
94.505	608.17	10	61.15	306.0	10
95.447	600.46	15	62.92	292.9	5
3502.588	542.15	10	63.42	289.1	10
16.468	429.49	30	68.10	254.3	10
39.326	245.89	10	70.79	234.3	5
70.730	27 997.48	2	71.41	229.7	5
70.886	996.26	5	71.62	228.2	5
92.114	830.82	5	72.00	225.4	2
3627.105	563.02	5	80.15	165.1	10
29.302	545.65	3	82.07	150.9	10
37.874	480.75	3	83.177	142.74§	70
40.237	462.91	2	84.113	135.85§	30
64.706	279.55	5	84.732	131.29§	50
64.792	278.91	5	85.943	122.38§	70
65.492	273.70	5	86.211	120.41§	40
67.551	258.38	5	88.554	103.18	5
68.244	253.24	2	3706.9	26 969	5
83.867	137.66	20	13.9	918	5
85.183	127.97	15	15.0	910	2
85.502	125.63	10	33.3	778	10
3794.917	26 343.56	2	41.1	723	10
3814.426	208.82	3	56.0	617	2
15.182	203.63	2	58.3	600	2
17.443	188.12	1	68.5	528	2
26.693	124.81	1	71.8	505	1
40.842	028.58	3	72.6	499	1
42.003	020.71	5	78.3	459	2
42.936	014.39	5	80.8	442	2
43.451	010.91	5	3923.4	25 481	2
45.266	25 998.63	5	25.5	467	2
47.639	982.60	2	36.1	399	2

$N_2{}^{16}O^+$			$N_2{}^{18}O^+$		
λ_{air}(head) (*a*)†	ν_{vac}(head) (*b*)	intensity (*d*)	λ_{air}(head) (*a*)	ν_{vac}(head) (*b*)	intensity (*d*)
3904.276	25605.69	1	3939.2	25379	2
05.977	594.41	1	45.6	338	2
4102.939	24365.90	2	47.0	329	2
04.874	354.41	1	48.5	319	2
			52.1	296	2
			66.7	203	1
			67.7	196	1
			70.0	182	1
			71.6	172	1
			91.4	047	1
			4001.8	24982	1
			04.9	962	1
			07.5	946	1
			14.2	905	1
			19.3	873	1

† Band heads are listed more or less in order of increasing wavelengths, except that those of a given vibronic transition are grouped together.

(*a*) Wavelengths quoted to three decimals (Å): from high-resolution plates. Two decimals: Bausch & Lomb 1.5 m Eagle grating, second order. One decimal: *ibid.*, first order.

(*b*) Wavenumbers (cm^{-1}) quoted to two decimals: from high-resolution grating plates. To one decimal or nearest whole number: 1.5 m grating in second and first orders respectively.

(*c*) Band centres (cm^{-1}) quoted to two decimals: from rotational analysis. To one decimal: from nearby Q-branch head frequency (*b*) and an estimate of the head-centre separation derived from approximate rotational constants (see text).

(*d*) On a visual scale of 100. It is not easy to relate these values to any absolute measures of transition-probabilities for they were obtained by comparing exposure times needed to bring up band heads containing variable numbers of unresolved lines to comparable intensities on photographic plates. They should therefore be regarded only as very rough relative estimates.

‡ Bands present but perturbed.

§ These bands are all part of the transition 1^0_1 in which ν''_1 is strongly perturbed.

PHILOSOPHICAL TRANSACTIONS OF THE ROYAL SOCIETY A MATHEMATICAL, PHYSICAL & ENGINEERING SCIENCES

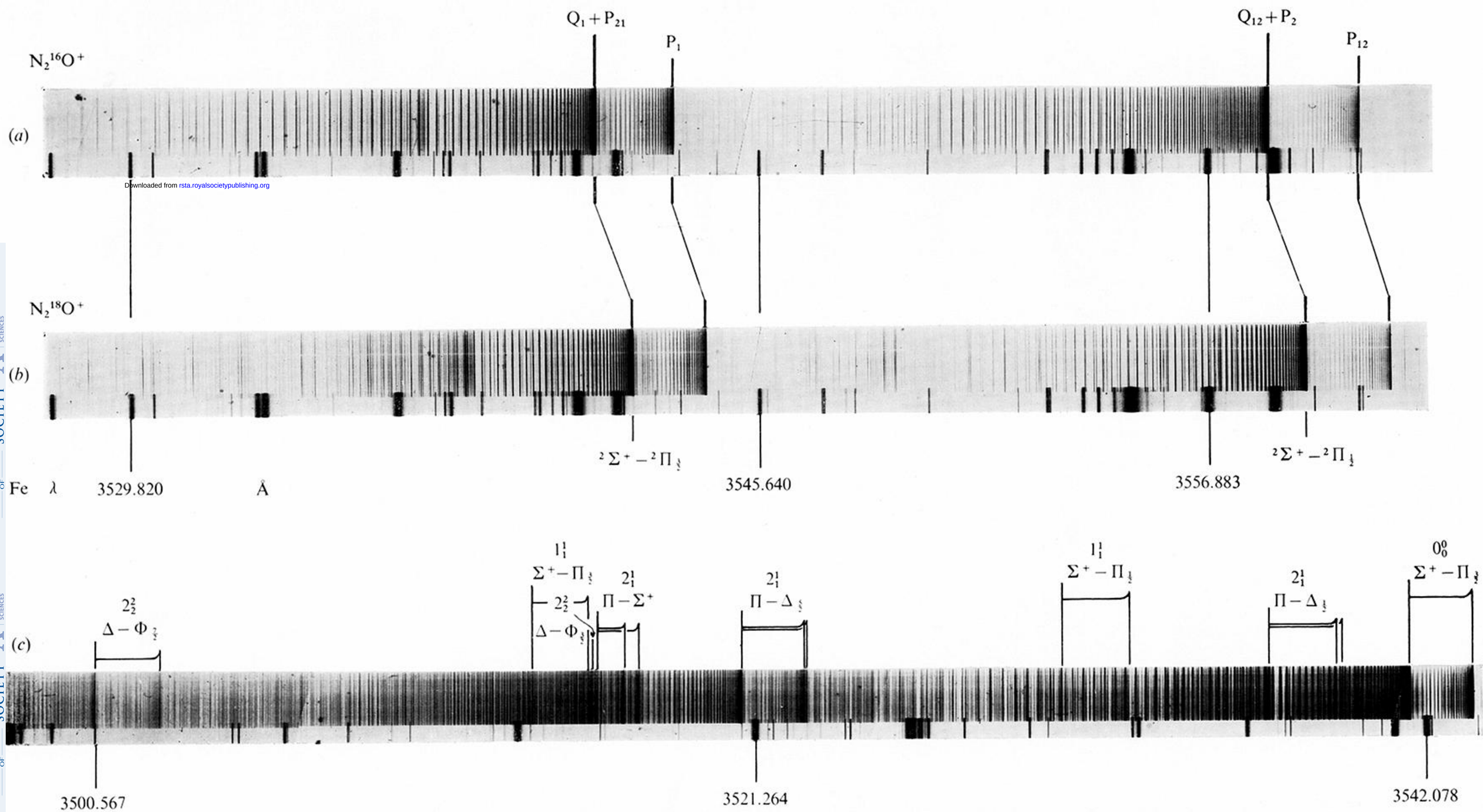

FIGURE 2. The (0, 0) band and sequences under high resolution.
(*a*) $N_2{}^{16}O^+$; (*b*) $N_2{}^{18}O^+$; (*c*) bands to the violet of the $^2\Sigma^+$–$^2\Pi_{\frac{3}{2}}$ component, $N_2{}^{16}O^+$.

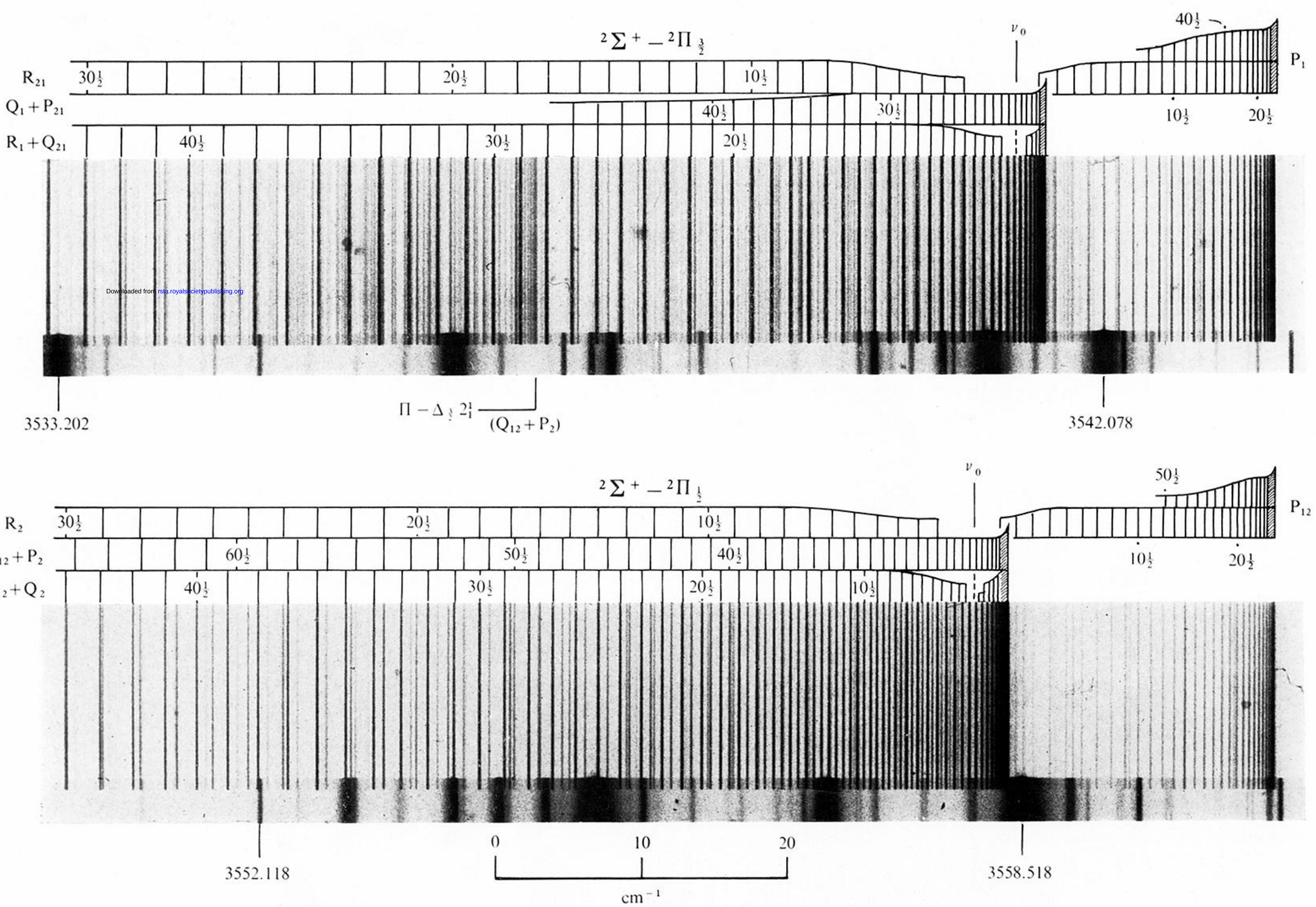

FIGURE 3. The (0, 0) band of $N_2{}^{16}O^+$, showing the rotational assignments of branches.